Discriminant Analysis for Severe Storm Environments in South-Central Brazil

LETÍCIA O. DOS SANTOS,[a] ERNANI L. NASCIMENTO,[a] AND JOHN T. ALLEN[b]

[a] *Grupo de Modelagem Atmosférica, Departamento de Física, Universidade Federal de Santa Maria, Santa Maria, Rio Grande do Sul, Brazil*

[b] *Department of Earth and Atmospheric Sciences, Central Michigan University, Mount Pleasant, Michigan*

(Manuscript received 17 December 2022, in final form 11 July 2023, accepted 24 July 2023)

ABSTRACT: Severe storms produce hazardous weather phenomena, such as large hail, damaging winds, and tornadoes. However, relationships between convective parameters and confirmed severe weather occurrences are poorly quantified in south-central Brazil. This study explores severe weather reports and measurements from newly available datasets. Hail, damaging wind, and tornado reports are sourced from the PREVOTS project from June 2018 to December 2021, while measurements of convectively induced wind gusts from 1996 to 2019 are obtained from METAR reports and from Brazil's operational network of automated weather stations. Proximal convective parameters were computed from ERA5 reanalysis for these reports and used to perform a discriminant analysis using mixed-layer CAPE and deep-layer shear (DLS). Compared to other regions, thermodynamic parameters associated with severe weather episodes exhibit lower magnitudes in south-central Brazil. DLS displays better performance in distinguishing different types of hazardous weather, but does not discriminate well between distinct severity levels. To address the sensitivity of the discriminant analysis to distinct environmental regimes and hazard types, five different discriminants are assessed. These include discriminants for any severe storm, severe hail only, severe wind gust only, and all environments but broken into "high" and "low" CAPE regimes. The best performance of the discriminant analysis is found for the "high" CAPE regime, followed by the severe wind regime. All discriminants demonstrate that DLS plays a more important role in conditioning Brazilian severe storm environments than other regions, confirming the need to ensure that parameters and discriminants are tuned to local severe weather conditions.

KEYWORDS: South America; Convective storms; Storm environments

1. Introduction

As in other parts of the world, severe storms can lead to damage to property, infrastructure, and crops, and in extreme cases, represent a threat to life in south-central Brazil. These storms can produce large hailstones (≥2 cm), damaging winds (≥90 km h^{-1}) and, less frequently, tornadoes. Any of these phenomena can result in significant social and economic impacts in both urban and rural areas. For example, a 2021 hailstorm in Bom Jesus, a city with 11 500 inhabitants in southern Brazil, caused in excess of the equivalent to $9.1 million (USD) in damage to crops (EMATER/ASCAR 2021). Despite this potential for impacts, the environments that favor the development of severe storms based on the prevailing atmospheric ingredients (hereafter severe storm environments) are poorly understood in this region owing to a lack of reliable severe weather reports. Two primary ingredients include the presence of conditional instability and moderate to intense vertical shear of the horizontal wind (Doswell et al. 1996).

In the past decade, a number of investigations have addressed deep convective storms over north-central Argentina, where they are strongly influenced by the local topography and are mostly associated with the occurrence of large hail (Romatschke and Houze 2010; Matsudo and Salio 2011; Rasmussen and Houze 2011; Rasmussen et al. 2014; Mulholland et al. 2018; Bruick et al. 2019). Results from these studies laid the scientific basis for an international field campaign called RELAMPAGO-CACTI (Nesbitt et al. 2021; Varble et al. 2021), with the goal of conducting intensive observation of convective storms in Argentina and extreme southern Brazil during the austral spring of 2018. Data collection strategies during RELAMPAGO-CACTI aimed mainly at the understanding of orographic influences on convective initiation and development, upscale growth of the convective activity, and cloud microphysics controlling hail production. Results from this field campaign are now being published (Borque et al. 2020; Kumjian and Lombardo 2020; Mulholland et al. 2020; Piersante et al. 2021; Schumacher et al. 2021; Bechis et al. 2022, among others).

In a similar timeframe to the development of research over Argentina, a number of studies have also explored severe weather in southern and southeastern Brazil (Silva Dias 2011; Nascimento et al. 2014; Ferreira and Nascimento 2016; Martins et al. 2017; Ribeiro and Seluchi 2019; Figueiredo et al. 2019; Ribeiro et al. 2019; Pereira Filho et al. 2019; Bender et al. 2019; Beal et al. 2020; Oliveira et al. 2022; Ferreira et al. 2022). These studies have addressed a variety of topics related to severe storms in the region, including description of significant cases, regional climatology of severe storms, the background synoptic and mesoscale environments, analysis of radar and satellite signatures, and the distribution of severe weather reports. However, no long-term climatology for severe storm environments exists for Brazil.

In the ingredients-based approach, proximity soundings are an important tool to understand the relationship between

Corresponding author: Letícia dos Santos, deoliveiraaicitel@gmail.com

DOI: 10.1175/MWR-D-22-0347.1

preconvective atmospheric conditions and the occurrence of severe convection (e.g., Rasmussen and Blanchard 1998; Brooks et al. 2003; Potvin et al. 2010; Púčik et al. 2015; Coniglio and Parker 2020). However, the frequency with which operational radiosondes are launched (most often, twice a day) and the typically poor spatial density of the upper-air stations in regions like south-central Brazil, strongly limit the opportunities for an actual sounding to meet the criteria for a proximity sounding (Brooks et al. 2003). In Brazil, there are twice-daily radiosonde launches at 0000 and 1200 UTC, with the lack of midafternoon (1800 UTC) soundings representing a significant limitation for sampling preconvective environments (e.g., Schumacher et al. 2021 shows the importance of 1800–2000 UTC soundings to convective storm environments in central Argentina during RELAMPAGO-CACTI intensive observing periods). Even if the actual soundings were sufficiently frequent, such data are linked to a specific location and may not be representative for the storm region (Potvin et al. 2010).

Reanalysis or model-derived proximity pseudosoundings can be used in order to overcome the difficulty of automated or conventional identification of a storm environment (Brooks et al. 2003; Coniglio and Jewell 2022). The grid points in proximity to storm reports are considered and generate a vertical profile similar to those derived from actual soundings (Allen et al. 2011; Allen and Karoly 2014; Gensini et al. 2014; Taszarek et al. 2018, 2021). For this study, the fifth generation of the European Centre for Medium-Range Weather Forecasts (ECMWF) global reanalysis data (ERA5; Hersbach et al. 2020) are employed to provide proximal profiles to severe storm reports.

A combination of indices is often considered to identify favorable conditions for severe storms environments and for discriminating between severe and nonsevere storms (Rasmussen and Blanchard 1998). For example, convective available potential energy (CAPE) and deep-layer shear have been analyzed in several convective storm environments studies as well as a number of other potential convective parameters (Brooks et al. 2003; Craven and Brooks 2004; Allen et al. 2011; Allen and Karoly 2014; Gensini and Ashley 2011; Sherburn and Parker 2014; Bruick et al. 2019; Taszarek et al. 2019, 2020, 2021). These previous studies motivate the use of such an ingredients-based approach in Brazil, where it has not been applied before with the availability of a high-quality database of severe weather reports.

Research on convective storm environments mostly has concentrated on specific domains, such as the United States (Brooks et al. 2003, 2007; Gensini and Ashley 2011; Gensini et al. 2014; Allen and Tippett 2015; Gensini and Brooks 2018; Tang et al. 2019; Li et al. 2020; Taszarek et al. 2020), Europe (Púčik et al. 2017; Rädler et al. 2018; Taszarek et al. 2018, 2019, 2020), Australia (Allen et al. 2011; Allen and Karoly 2014), South Africa (Blamey et al. 2017), China (Li et al. 2018), and Argentina (Bruick et al. 2019), with some also encompassing a global perspective (Brooks et al. 2003; Zipser et al. 2006; Prein and Holland 2018; Glazer et al. 2021; Taszarek et al. 2021). All these global investigations found that subtropical South America, east of the Andes mountain range (including north-central Argentina, Paraguay, Uruguay, and southern Brazil) is one of the world's "hotspots" for severe convective activity.

The lack of a discriminant function between nonsevere and severe storm environments based on actual ground-based convective storm reports for South America is the motivation for the present study. Recently, a voluntary initiative called *Plataforma de Registros e Rede Voluntária de Observadores de Tempestades Severas* (PREVOTS) (Portuguese for Storm Spotting Network and Platform for Severe Weather Reports), led by a group of Brazilian meteorologists, has developed a severe storm database that comprises reports from the last 4.5 years in Brazil. Although it does not provide a sufficiently long historical record to establish a comprehensive severe weather climatology for this region, this database provides an opportunity to develop an independent discriminant function between nonsevere and severe storm environments, which, to date, has not been explored.

The robust nature of the new PREVOTS dataset, together with the availability of high-resolution ERA5 reanalysis data allows development of a unique proximity pseudosounding study for severe events in Brazil. The goal of this discriminant approach is to improve the climatological knowledge of these environments over portions of the La Plata basin region. The following specific questions are addressed by the present study: 1) Are existing discriminants (referring to CAPE/shear regimes) sufficient to characterize observed severe convective environments in this region? 2) How are observed severe weather reports in the region related to their environment? 3) What do independently derived discriminants look like? These discriminants are developed with the future goal to estimate and evaluate the overall climatology of severe storm environments over longer periods in the past and also for the future under different climate change scenarios for this region.

2. Data and methods

a. *PREVOTS database*

The goal of the PREVOTS project (https://prevots.org) is to create a network of Brazilian storm spotters, as well as a consolidated database consisting of high-quality severe weather reports from Brazil. The dataset provides detailed and quality-controlled information on weather events associated with severe convective storms over Brazil. This initiative follows the example of the European Severe Weather Database (ESWD, https://eswd.eu), which started operational service in 2006 and is hosted by the European Severe Storms Laboratory (ESSL).

Reports from social media, news media, governmental institutions, and volunteer storm spotters are used to construct the database. The information made available by this initiative includes the date, local time, municipality and state, latitude and longitude, type of severe convective weather (hail, damaging winds, or tornado), a description about the source of the report, existence of photos and/or videos, news links (if available), detailed damage information (whenever available), and how the time of occurrence was determined/estimated. The intensity or size of the respective phenomenon is also provided, even if estimated (hail size in cm, winds in km h^{-1}). All

TABLE 1. Summary of observations and weather reports available for this study. The first column indicates the categories and sources of the weather reports/observations. All hail reports come from the PREVOTS database. The second column informs the full sample size of each corresponding category/source. The third column indicates the number of proximity pseudosoundings obtained from the ERA5 global reanalysis corresponding to each category/source containing quantitative information about the weather occurrences.

Category	All reports/observations	ERA5 proximity soundings
Hail (no size info)	6290	—
Hail (<2 cm)—nonsevere	1380	871
Hail (≥2 cm)—severe	2180	1333
$\text{Wind}_{\text{PREVOTS}}$ (no speed info)	10 832	—
$\text{Wind}_{\text{PREVOTS}}$ (≥80 and <90 km h^{-1})—nonsevere	458	208
$\text{Wind}_{\text{PREVOTS}}$ (≥90 km h^{-1})—severe	375	188
$\text{Wind}_{\text{DECEA+INMET}}$ (≥54 and <90 kmh^{-1})—nonsevere	19 055	17 603
$\text{Wind}_{\text{DECEA+INMET}}$ (≥90 km h^{-1})—severe	1063	978
Tornado	200	39
Total	41 833	21 220

reports are manually checked to ensure quality. If the source of a storm report does not contain information about the time of occurrence, the time is estimated using radar or satellite imagery and an uncertainty in time is attributed to the report. The coordinates (latitude and longitude) of a report are also linked to uncertainty, i.e., the report occurred within a given distance from the attributed coordinates (B. Ribeiro 2023, personal communication). This methodology is inspired by the ESWD.

If there is a photo/video, the magnitude for hail reports is defined by its maximum diameter in centimeters (the description section states if the size was measured or estimated). However, not all hail reports have size information, as measurements or photo/video are not always available. Reports of severe wind gusts refer either to measured wind gusts greater than 80 km h^{-1} (approximately 22 m s^{-1}) or to wind damage associated with the passage of a convective storm. The intensity of wind gusts is not estimated, so, only measured winds have this information. Reports of waterspouts are considered tornadoes in the PREVOTS database, but a "waterspout" remark is added to the description section. No tornado report has an associated EF rating since a detailed poststorm damage assessment seldom is available.

Approximately 6000 reports have been collected on average each year since June 2018, with a total of 27 438 convective storm reports through the end of 2022. However, as many reports were associated with the same weather event, only about 12% of these reports (2639) were associated with unique ERA5 vertical profiles. The classification of the reports into nonsevere and severe categories is found in Table 1. Only reports with size or gust information were considered for the analysis of ERA5 atmospheric profiles. Further details on how reports were related to ERA5 vertical profiles are described in the proximity pseudosoundings section. Figure 1a shows the distribution of PREVOTS reports between 42°–58°W longitude and 18°–34°S latitude, totaling 16 529 reports from June 2018 to December 2021. This region is where severe convective storms are most frequent in Brazil, with atmospheric conditions sharing similar characteristics to those observed in north-central Argentina, Paraguay, and Uruguay, a known hot spot for severe deep convection (Zipser et al. 2006; Rasmussen et al. 2014; Taszarek et al. 2021).

One critical aspect regarding the use of reports of severe weather for atmospheric research is the existence of nonmeteorological factors that influence the number, quality, and geographical concentration of the reports, such as differences in procedures to collect the reports, and spatial inhomogeneities in population (Brooks 2013). For example, Silva Dias (2011) identified a dependence of the number of tornado reports on population density in Brazil. This study does not aim at addressing the influence of all these nonmeteorological factors on the sampling of severe weather reports, but the employment of reports made available by the PREVOTS database, which applies homogeneous procedures for collection and quality-control of the reports, should reduce the uncertainties in the source of severe weather information. This Brazilian database of in situ storm reports is a useful development and provides many research opportunities that were unavailable previously for this region.

b. *Convectively induced wind database*

The database of convectively induced wind gusts originally generated by Vallis et al. (2019) also was included in this study to increase the sample size. This database combines two sources of direct surface observations of convective wind gusts equal to or above 15 m s^{-1} coming from nationwide observing networks. The first source consists of METAR/SPECI/SYNOP aerodrome reports made available by the Departamento de Controle do Espaço Aéreo (DECEA; Department of Airspace Control) from the Brazilian Air Force covering the period from 1996 to 2019. The second source includes observations from the network of automated weather stations belonging to the Instituto Nacional de Meteorologia (INMET; Brazil's National Meteorological Institute) from 2000 to 2019. To be included in the INMET sample, the automated surface station must have operated for at least two years within this period. For simplicity, the two networks hereafter will be referred to as DECEA+INMET. Figure 1c displays the DECEA+INMET network in south-central Brazil, comprising a total of 216 INMET stations and 30 METAR/SPECI/SYNOP stations. Table 1 also summarizes the number of convectively induced wind gust measurements

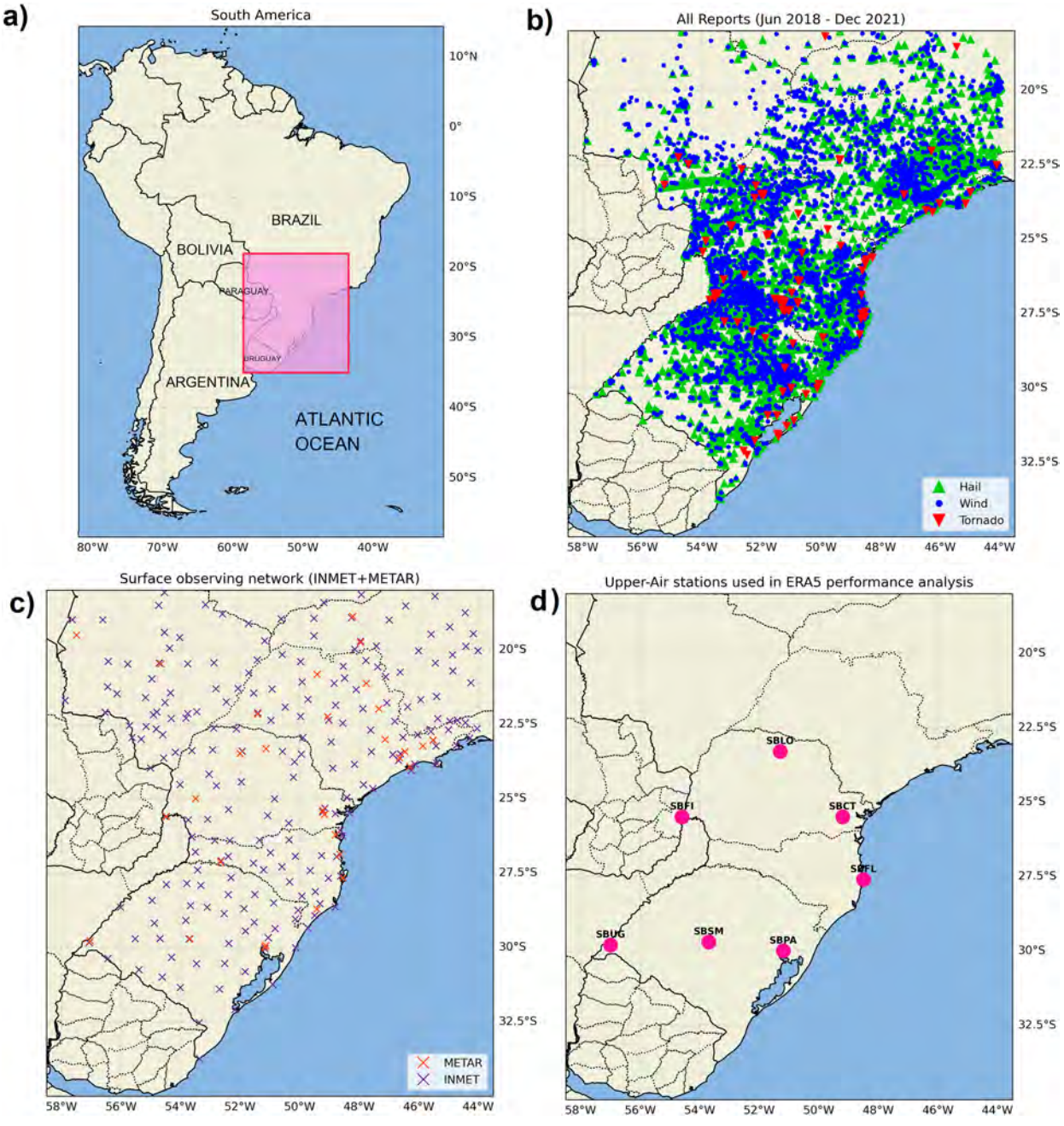

FIG. 1. Maps showing (a) the domain of interest in southeastern South America, enclosed by a pink box and (b) the spatial distribution of 16 529 severe weather reports within the domain of interest (42°–58°W, 18°–34°S) from the PREVOTS database between 1 Jun 2018 and 31 Dec 2021. (c) As in (b), but for the spatial distribution of METAR stations (DECEA in orange) and automated surface weather stations (INMET in purple) from Vallis et al. (2019) database of measured wind gusts. (d) Upper-air stations used in the ERA5 performance analysis (more details in Table 3).

coming from the DECEA+INMET dataset, separated by severe and subsevere categories. As in Lagerquist et al. (2017), it is assumed that none of the gust observations was produced by tornadic winds given the very low probability that an anemometer will sustain a direct hit from a tornado.

c. *Reanalysis data and convective parameters*

Considering the absence of frequent upper-air observations, most severe weather events around the world occur with no proximity sounding (Brooks 2013). Proximity soundings, when available, assist forecasters to identify atmospheric

conditions that are prone to the development of severe storms (Rasmussen and Blanchard 1998). Given the scarce number of proximity soundings for severe convective weather, especially outside of the United States, other sources of atmospheric information have been employed to characterize severe convective environments, such as global reanalysis data (Blamey et al. 2017; Glazer et al. 2021; Varga and Breuer 2022). The primary reason for using global reanalysis data is that they are uniformly distributed through time and space and cover all points on Earth, unlike in situ upper air observations. Atmospheric profiles extracted from reanalysis gridded data can provide information from a grid point nearest to the event of interest, allowing for the identification of larger number of profiles that meet the proximity criteria (Potvin et al. 2010). Although data from reanalyses are not an exact substitute for actual soundings, they can be useful when and where observations are scarce or simply not available (Brooks et al. 2003).

The vertical resolution provided by measurements from actual soundings allows for a more realistic representation of the atmospheric boundary layer as compared to the typical vertical resolution available from numerical products (e.g., Coffer et al. 2020; Coniglio and Jewell 2022). As the computation of some vertically integrated convective parameters (e.g., CAPE, storm-relative helicity) are highly sensitive to temperature, moisture, and wind profiles, especially at low levels, the vertical resolution issue can represent a source of inaccuracy for the calculation of these parameters (Taszarek et al. 2018). Additionally, for any numerical product, the representation of boundary layer and surface processes, crucial in affecting the magnitude of convective parameters, is influenced by choices of model discretization, physics parameterization schemes, and assimilation techniques (Allen and Karoly 2014; Li et al. 2020). In an ingredients-based approach, all the factors mentioned above contribute to inaccuracies in the representation of convective environments. Another relevant issue is that mechanisms for convective initiation are not represented by soundings. Moreover, there is no specific threshold in the convective parameter space capable of discriminating perfectly between severe and nonsevere storm environments (Doswell and Schultz 2006). Then, this approach enables the representation of an environment favorable to developing a severe storm and not the storm itself.

In this study, the atmospheric environments associated with the convective weather reports and observations in south-central Brazil are investigated utilizing tropospheric profiles obtained from the fifth generation of the ECMWF global reanalysis (ERA5), from which a number of convective parameters are computed. Horizontal and temporal resolution of the ERA5 reanalysis are 0.25° and 1 h, respectively, with data available on 137 hybrid-sigma vertical levels. Previous reanalysis products, such as ERA-Interim (80-km horizontal grid spacing and 60 vertical levels), MERRA-2 (50-km horizontal grid spacing and 60 vertical levels), and CFSR (38-km horizontal grid spacing and 64 vertical levels) were produced at a relatively low spatial resolution when compared to the ERA5 reanalysis. These improvements in resolution allow a better depiction of small-scale features that affect convective environments. Indeed, as evaluated by Taszarek et al. (2021), the ERA5 reanalysis is considered one of the best available tools for studying climatologies of convective parameters.

The choice of thermodynamic and kinematic parameters analyzed in this study was based on prior studies exploring convective environments around the world (Brooks et al. 2003; Allen et al. 2011; Púčik et al. 2015; Taszarek et al. 2020; Lepore et al. 2021; Zhou et al. 2021). Vertical profiles were produced over the south-central Brazil domain (Fig. 1) from pressure, temperature, specific humidity, and zonal and meridional (u and v) winds on ERA5's native hybrid-sigma vertical coordinates. For the calculation of parameters the xcape Python package was used (https://github.com/xgcm/xcape). CAPE and CIN were computed for different air parcels, including the 100 hPa mixed-layer (ML), most unstable (MU), and surface-based (SB) parcels. For simplicity, CIN is expressed as a positive quantity, rather than negative. Lifting condensation levels were calculated using the Stull approximation (Stull 2000). Storm relative helicity was calculated for the 0–1-km (SRH1) and 0–3-km (SRH3) layers using storm motions inferred from the Bunkers technique, and considering the mean 0–6-km unweighted wind speeds and the left-moving storm propagation (Bunkers et al. 2000). Lapse rates were obtained by vertical interpolation to the appropriate above-ground level (AGL) or pressure reference heights [2–4-km lapse rate, 700–500-hPa lapse rate (LR700-500)], while bulk vertical wind shears (of u and v) were likewise calculated [from the "surface" to 1 km, denoted low-layer shear (LLS) and from the "surface" to 6 km, denoted deep-layer shear (DLS), where "surface" is the lowest ERA5 reanalysis model level].

Recently, Varga and Breuer (2022) found that the ERA5 reanalysis performs well in representing convective parameters computed from its native hybrid-sigma vertical coordinate for central Europe, with high correlation coefficients for multiple variables and low error characteristics. They found that the MLCAPE computation based on the native ERA5 vertical coordinate showed improvement compared to the computation based on pressure levels. Moreover, they identified the smallest magnitude of underestimation for DLS, with the intensity of this error decreasing with increasing layer depth.

To evaluate the performance of ERA5 in representing general atmospheric profiles observed in southern Brazil, data from actual 0000 and 1200 UTC soundings for the 1996–2018 period from the operational network of upper air stations described in Table 2 and shown in Fig. 1d were obtained through the University of Wyoming weather website (https://www.weather.uwyo.edu/upperair/sounding.html). Following Nascimento et al. (2016), a quality control procedure was applied to the observations, after which a total of 65 786 actual soundings remained; Table 3 informs the number of quality-approved soundings per observation site. For each time and location of the actual soundings, a proximal vertical profile was obtained from ERA5 in its native vertical coordinate. Next, the two main convective parameters analyzed in this study, namely, MLCAPE and DLS, were computed for the two datasets to examine how well ERA5 reanalysis performs compared to CAPE and DLS observations in southern Brazil. Basic statistics, such

TABLE 2. Upper air stations used for the evaluation of ERA5 in representing general tropospheric profiles observed in southern Brazil. The last column informs the number of available soundings (considering 0000 and 1200 UTC).

Station	ICAO code	Lat (°S)	Lon (°W)	Elev (m)	Quality-approved soundings
Londrina	SBLO	23.3	51.3	569	6352
Curitiba	SBCT	25.5	49.2	908	11 713
Foz do Iguaçu	SBFI	25.5	54.6	180	10 262
Florianópolis	SBFL	27.6	48.5	5	10 041
Santa Maria	SBSM	29.7	53.7	85	7901
Uruguaiana	SBUG	29.8	57.0	74	6496
Porto Alegre	SBPA	30.0	51.2	3	13 021

as the Pearson correlation coefficient, root-mean squared error, and mean absolute error Wilks (2011), were computed to assist in the objective assessment of ERA5's performance.

d. *Proximity pseudosoundings*

Tropospheric profiles were obtained from ERA5 reanalysis to serve as proximity pseudosoundings by selecting grid points nearest to each hail or wind report from PREVOTS and to each DECEA+INMET wind measurement, and hourly data closest to the time of the respective report/measurement. To that end, only PREVOTS reports containing information about hail size or wind speed and DECEA+INMET measurements were considered, because only those allowed the distinction between severe events (hail diameter equal to or greater than 2 cm, or wind speed equal to or greater than 25 m s^{-1}) and nonsevere events (hail diameter or wind speed not reaching the aforementioned thresholds). Tornado reports were not included because its small sample would not contribute to the statistical significance of the results.

To ensure that the environments being sampled reflected independent events and were not duplicates for the same event, filtering criteria were applied to the PREVOTS reports and DECEA+INMET measurements. First, when a pair or a cluster of PREVOTS reports was found for the same selected grid point at exactly the same hour, only one report was considered representative of that grid point/time selection, that being the report associated with the largest hail report or strongest wind gust among all reported phenomena. Similarly, if two DECEA+INMET gust measurements coincided for the same location and time, the strongest gust was selected. As an additional criterion for obtaining the pseudosoundings from ERA5, PREVOTS reports valid for the same ERA5 time but removed less than three grid points from each other, or associated with the same ERA5 grid point but being less than 2 h apart from each other, were considered as one same event for which one single tropospheric profile was obtained, being the one with highest MLCAPE. Differing from Brooks et al. (2003) and Allen et al. (2011), tropospheric profiles displaying MLCAPE less than 100 J kg^{-1} (but above 1 J kg^{-1} and with DLS greater than 1 m s^{-1}) were maintained in the sample and defined as "low-CAPE" environments. After applying these filtering criteria, a total of 21 220 proximity pseudosoundings were obtained from the ERA5 reanalysis (Table 1), representing an adequate sample size for a statistical analysis that aims at developing a discriminant function for severe and nonsevere weather environments.

e. *Linear discriminant analysis*

Following an ingredients-based approach, Brooks et al. (2003) determined a discriminator for diagnosing significant severe and severe thunderstorm environments around the world based mainly on a combination of conditional instability (CAPE) and DLS (0–6-km bulk wind difference) applied to the National Centers for Environmental Prediction (NCEP) global reanalysis data. Similarly, Allen et al. (2011) established a regional discriminant to distinguish between severe and

TABLE 3. Skill scores, where POD = probability of detection, POFD = probability of false detection, CSI = critical success index, HSS = Heidke skill score, TP = true positive, TN = true negative, FP = false positive, FN = false negative, ET = expected true, N = total.

Skill score	Defined by	Question	Perfect score
Accuracy	$\frac{TP + TN}{N}$	What fraction of the forecasts were correct?	1
POD	$\frac{TP}{TP + FN}$	What fraction of the observed "yes" events were correctly forecast?	1
POFD	$\frac{FP}{TN + FP}$	What fraction of the observed "no" events were incorrectly forecast "yes"?	0
CSI	$\frac{TP}{TP + FN + FP}$	How will did the forecast "yes" events correspond to the observed "yes" events?	1
HSS	$\frac{(TP + TN) - (ET)_{random}}{N - (ET)_{random}}$	What was the accuracy of the forecast relative to that of random chance?	1

significant severe storm environments for Australia using Mesoscale Limited Area Prediction System (MesoLAPS) proximity soundings. Later, Allen and Karoly (2014) modified this discriminant to assess the frequency of severe thunderstorm environments in Australia based on proximal pseudosoundings obtained from the ERA-Interim reanalysis. Adopting this general methodology, a considerable number of studies developed regionally tuned discriminators based on CAPE and DLS computed from reanalysis products or regional climate models to address the climatological distribution and frequency of severe storm environments in different parts of the world (Glazer et al. 2021; Taszarek et al. 2019, 2020). With the availability of severe and nonsevere weather reports and observations for south-central Brazil and the corresponding proximity pseudosoundings obtained from ERA5 reanalysis, this work aims at conducting a discriminant analysis based on CAPE and DLS to distinguish severe from nonsevere storm environments for that region.

One limitation is that, as described in the previous subsection, nearly 90% of the ERA5 pseudo proximity soundings are associated with reports or measurements of wind gusts. This makes the sample of atmospheric environments biased toward one specific category of weather phenomenon, namely, the convectively induced winds. This is a particularly relevant aspect because, while large hail and intense tornadoes are strongly tied to the supercellular mode of deep convection (for which a covariate consisting of CAPE and DLS is generally appropriate to distinguish between favorable and unfavorable environments; Brooks et al. 2003), strong convective wind gusts can occur in association with a much wider spectrum of storm organization. This includes multicells, mesoscale convective systems, supercells, and even rather disorganized convective activity (e.g., Smith et al. 2013; Romanic et al. 2022). Therefore, it is likely that the sample of pseudo proximity soundings predominantly related to reports/measurements of convective wind gusts comprises atmospheric environments that are more diverse than those related to large hail and mesocyclone tornadoes (supercell environments). Beyond proximal environments, cloud microphysics processes also play a key role in driving convective downdrafts associated with surface wind gusts. As such, the parameter space consisting of CAPE and DLS may be rather limited to allow for a strong discrimination between severe and nonsevere convective environments based on our sample. While not hindering the employment of this sample for the discriminant analysis being proposed, caution will be necessary regarding generalization of the findings in the context of severe convective weather.

The linear discriminant analysis was performed (Fisher's linear discriminant; Wilks 2011) using the sample available from PREVOTS reports and DECEA+INMET networks. The linear discriminant analysis (LDA) approach seeks to find the axes that maximize the separability among known classes and minimizes the variation within each category. The LDA is a linear transformation technique, a supervised form of machine learning used to distinguish two classes or groups. Data were first split into 20% for testing and 80% for training datasets, using a stratified split method where the data are shuffled. To quantify the uncertainty of the results, discriminants were computed using 10 iterations of 10 resampled subsamples. This results in 10 values, one for each subsample. The final discriminant was chosen based on the central function between the maximum and minimum discriminants. This discrimination model was developed using Python's scikit-learn library (Pedregosa et al. 2011). To evaluate model performance, a series of skill scores were used (Table 2). They were computed for each of the central point discriminants and their range is the distance of this central point to the maximum and minimum functions.

3. Results

a. *ERA5 performance for the convective parameters in south-central Brazil*

Considering that a performance evaluation of ERA5 in representing convective parameters has not been previously explored for south-central Brazil, this section provides an overview of such an assessment. As indicated in Fig. 2, DLS is generally better estimated than MLCAPE by ERA5, possibly due to vertical resolution limitations, parameterization schemes, and assimilation techniques (Taszarek et al. 2018; Allen and Karoly 2014). This is similar to the performance of other reanalysis datasets (Taszarek et al. 2018; Varga and Breuer 2022). The correlation coefficient is lower and errors are higher for DLS in south-central Brazil when compared to Europe and the United States (Taszarek et al. 2018; Varga and Breuer 2022). ERA5-derived MLCAPE in south-central Brazil has a higher correlation with real soundings when compared to the Pannonian basin region in Europe (Varga and Breuer 2022), but lower when compared to the United States and Europe (Taszarek et al. 2018). However, MAE and RMSE for MLCAPE in south-central Brazil are higher compared to Varga and Breuer (2022) and lower compared to Taszarek et al. (2018), which can be related, respectively, to lower and higher MLCAPE values in these regions.

Box-and-whisker plots for MLCAPE in Fig. 3a shows quite similar distributions of interquartile ranges. Differences are seen for higher percentiles when ERA5 reanalysis tends to underestimate MLCAPE. DLS is also slightly underestimated by ERA5 reanalysis (Fig. 3b). This result is consistent with other reanalyses that were compared with soundings in the United States and Europe (Taszarek et al. 2018; Varga and Breuer 2022).

The main point from the above evaluation is that the ERA5 reanalysis data are able to properly reproduce the statistics observed in CAPE and DLS values for south-central Brazil. Therefore, the convective parameters (at least those involving CAPE and DLS) extracted from ERA5 profiles are adequate for the development of this and future studies regarding the climatology of severe storm environments for this region.

b. *Monthly and diurnal distribution of severe events*

To reorient Northern Hemisphere readers, it is important to mention that seasons here are presented in a Southern Hemisphere context. The monthly distribution of nonsevere and severe weather reports in south-central Brazil (Fig. 4a)

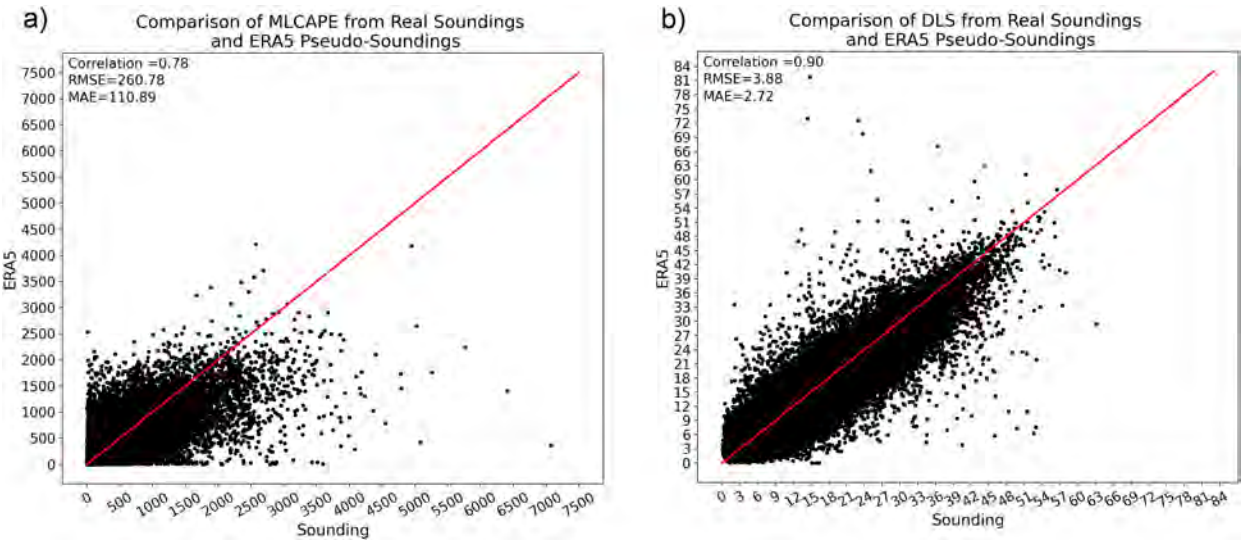

FIG. 2. Comparison of actual soundings with ERA5 pseudo soundings for (a) MLCAPE and (b) DLS. The red line denotes a one-to-one ratio. Scores in the top-left corner of each plot are the Pearson correlation coefficient, root-mean-square error, and mean absolute error.

exhibits a favorable peak between spring and summer, with an increasing number during the end of winter and early summer. Autumn has the lowest frequency, with the period between March and May explaining about 16% of the total annual reported events. The large increase in severe events in October (Fig. 4a) is similar to supercell climatologies for central Argentina (Mulholland et al. 2018; Piscitelli et al. 2022). The results presented here also agree with those presented for destructive hail storms in Brazil (Martins et al. 2017) and in the triple border of Brazil, Argentina, and Paraguay (Beal et al. 2020). The monthly distribution only for hail occurrences (Fig. 4b) is partly consistent with the remotely sensed climatology by Cecil and Blankenship (2012): autumn and early winter exhibit the least active period, but from late winter on, hail events again increase. Specifically for severe wind and tornado, the most frequent months of occurrence are October and June, respectively, although the wind cases also present an overall peak of occurrence between midspring to early summer.

Diurnally, the highest frequency of convective storms in south-central Brazil is found in the midafternoon (Fig. 5a), consistent with other regions, reflecting the maximization of intense diurnal heating in this predominantly subtropical region. A weaker peak can be observed during the period between 1800 and 2200 local time (LT), suggesting that another mechanism could be playing an important role in convective

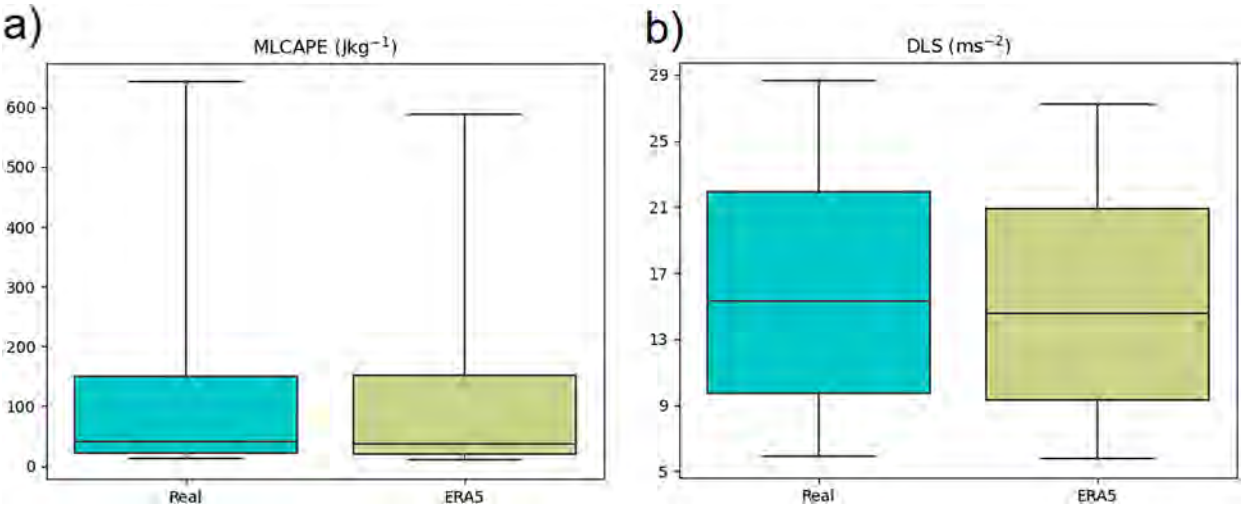

FIG. 3. Box-and-whisker plots for actual soundings (light blue) and ERA5 pseudosoundings (olive) for (a) MLCAPE and (b) DLS. The median is represented as a horizontal line inside the box, the edges of the box represent the 25th and 75th percentiles, and the whiskers represent the 10th and 90th percentiles.

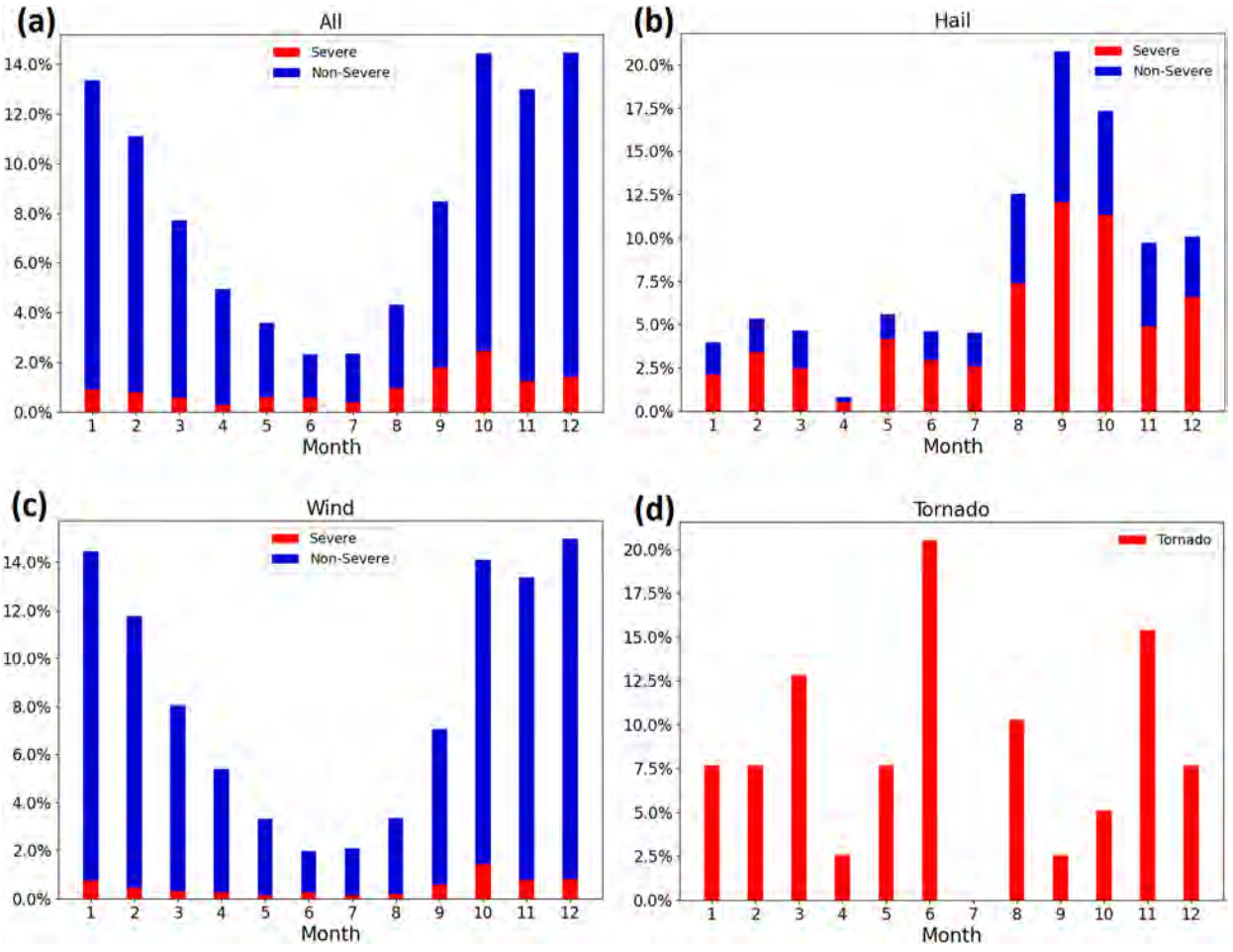

FIG. 4. Monthly relative frequency of (a) all categories, (b) hail, (c) wind, and (d) tornado reports. Severe is indicated in red and nonsevere is indicated in blue. Note different value scales in ordinates.

storms in this region, similar to the factors noted in Argentina (Bruick et al. 2019). In fact, some studies (Salio et al. 2007; Anabor et al. 2008) describe that southern Brazil (part of the domain analyzed here) has a high frequency of mesoscale convective systems (MCS) reaching maturity in the late night.

c. *Convective parameters*

Results of parameter distribution are discussed through the analysis of box-and-whisker plots. The main purpose of the statistics is to describe the magnitude and to provide objective criteria to identify, among the full sample of events, the profiles that are potentially indicative of severe weather environments. To show the difference between environments in distinct events according to their intensity classes, the nonparametric Mann–Whitney U test, with a two-tailed significance level of $p < 0.05$ (or 95% confidence level) was applied (Table 4).

1) THERMODYNAMIC PARAMETERS—INSTABILITY

Figure 6 shows that in particular for hail cases (both nonsevere and severe), values of MLCAPE are very similar to those found by Taszarek et al. (2020) for Europe. In contrast, MLCAPE is substantially lower than observed in the United States and near the Sierras de Córdoba (Mulholland et al. 2018), even when a "high-shear low-CAPE" U.S. environment is considered (Sherburn and Parker 2014). For all types of convective weather, there are large overlaps between the different intensities. However, the statistically significant separation between intensities at a 95% confidence interval (Table 4) suggests that MLCAPE and MLLCL are efficient predictors for hail and poor for wind, whereas LR700-500 works better to discriminate wind intensities instead of hail climatology.

In terms of wind, MLCAPE in Brazilian cases is considerably lower compared to both Europe and the United States. Considering tornado environments, more than half of 39 cases had less than 600 J kg^{-1}, which is very similar to those classified as F2 and F3 in Europe (Taszarek et al. 2020) and to Australian cool season tornado environments (Allen et al. 2021). However, when compared to tornado environments in the United States (Thompson et al. 2012) and warm season cases in Australia, Brazilian tornado environments have considerably lower MLCAPE values.

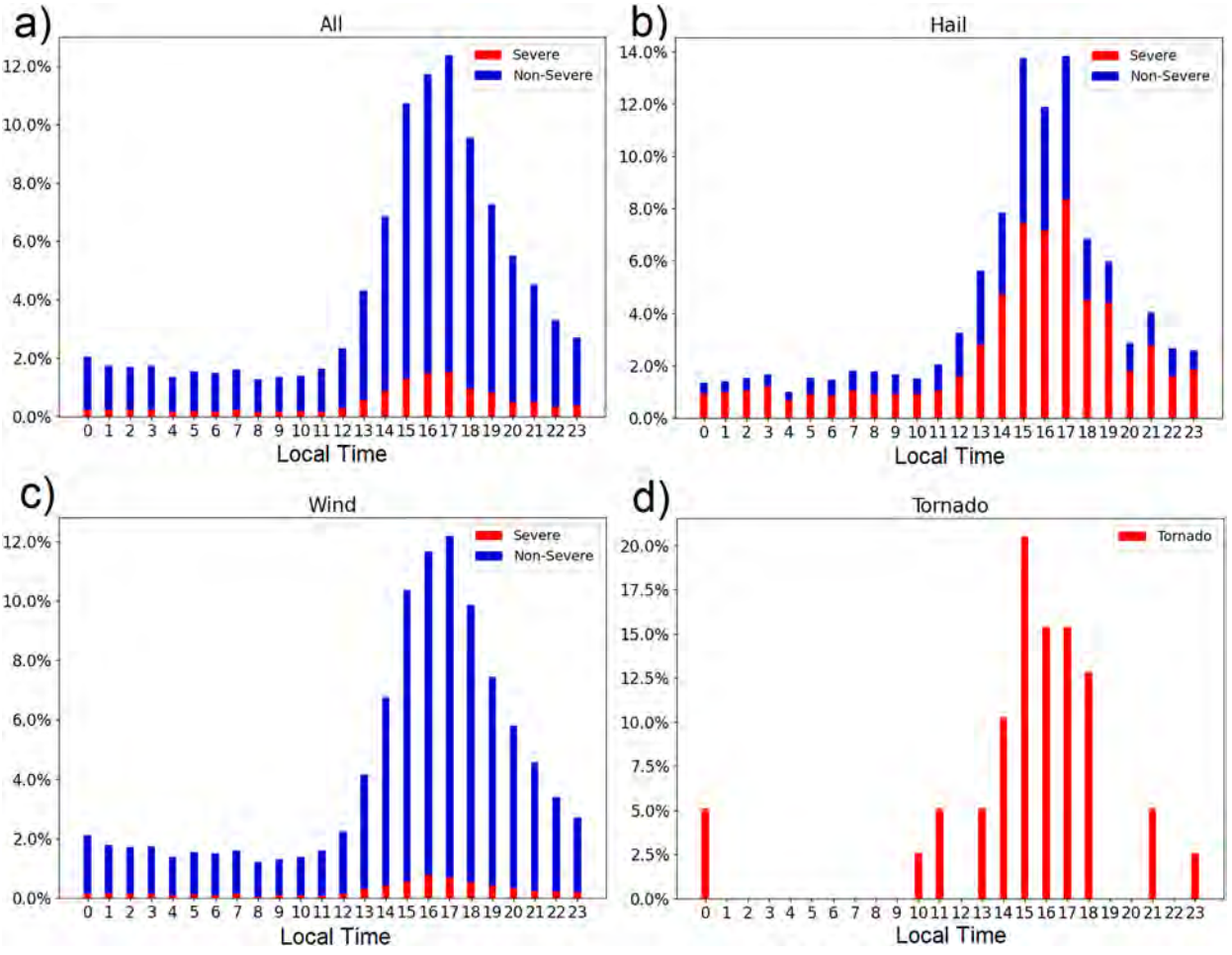

FIG. 5. Diurnal relative frequency of (a) all categories, (b) hail, (c) wind, and (d) tornado reports. Severe is indicated in red and nonsevere is indicated in blue. Note different value scales in ordinates.

A more general relationship between the strength of the MLCIN and severity is presented in Fig. 6b. The severe hail and wind environments had slightly greater median and upper quartile MLCIN absolute values compared to the nonsevere, and despite the interquartile ranges overlapping, convective inhibition does satisfactory work of separating nonsevere to severe hail and wind (see p values in Table 4). For tornado environments, variability in MLCIN is smaller compared to hail and wind, indicating that tornadoes can form in a restricted range of MLCIN environments.

Lower MLLCL values are observed in south-central Brazil when compared with those over Europe and the United

TABLE 4. The p values derived from the Mann–Whitney U test. The results are statistically significant at the 95% confidence interval if $p < 0.05$ (bolded). TSUR = temperature at 2 m; HNS = hail nonsevere; HS = hail severe; WNS = wind nonsevere; WS = wind severe; 1—group of MLCAPE lower than 100 J kg^{-1}; 2—group of MLCAPE greater than 100 J kg^{-1}. The p values for MLCAPE between groups 1 and 2 were omitted due to their definition.

Parameter	HSxHNS	WSxWNS	HNS1xHNS2	HS1xHS2	WNS1xWNS2	WS1xWS2
MLCAPE	$\mathbf{2.18 \times 10^{-4}}$	0.7430	—	—	—	—
DLS	$\mathbf{1.97 \times 10^{-10}}$	$\mathbf{4.31 \times 10^{-45}}$	$\mathbf{7.38 \times 10^{-48}}$	$\mathbf{3.31 \times 10^{-53}}$	**0.00**	$\mathbf{9.48 \times 10^{-22}}$
MLCIN	$\mathbf{7.09 \times 10^{-7}}$	$\mathbf{2.14 \times 10^{-23}}$	$\mathbf{5.68 \times 10^{-37}}$	$\mathbf{6.17 \times 10^{-32}}$	$\mathbf{6.28 \times 10^{-35}}$	0.9099
MLLCL	**0.0041**	0.6217	$\mathbf{1.19 \times 10^{-6}}$	$\mathbf{3.03 \times 10^{-7}}$	$\mathbf{7.85 \times 10^{-51}}$	**0.0084**
LR700-500	0.2571	$\mathbf{4.44 \times 10^{-24}}$	0.2064	0.4778	$\mathbf{6.69 \times 10^{-23}}$	0.3722
LLS	**0.0001**	$\mathbf{5.96 \times 10^{-32}}$	$\mathbf{7.80 \times 10^{-22}}$	$\mathbf{8.74 \times 10^{-18}}$	$\mathbf{2.09 \times 10^{-199}}$	$\mathbf{2.30 \times 10^{-14}}$
SRH3	$\mathbf{3.72 \times 10^{-8}}$	$\mathbf{3.46 \times 10^{-39}}$	$\mathbf{1.03 \times 10^{-42}}$	$\mathbf{5.97 \times 10^{-42}}$	$\mathbf{3.86 \times 10^{-190}}$	$\mathbf{7.21 \times 10^{-18}}$
TSUR	0.1152	$\mathbf{2.77 \times 10^{-5}}$	$\mathbf{1.40 \times 10^{-52}}$	$\mathbf{1.67 \times 10^{-71}}$	**0.00**	$\mathbf{8.48 \times 10^{-31}}$

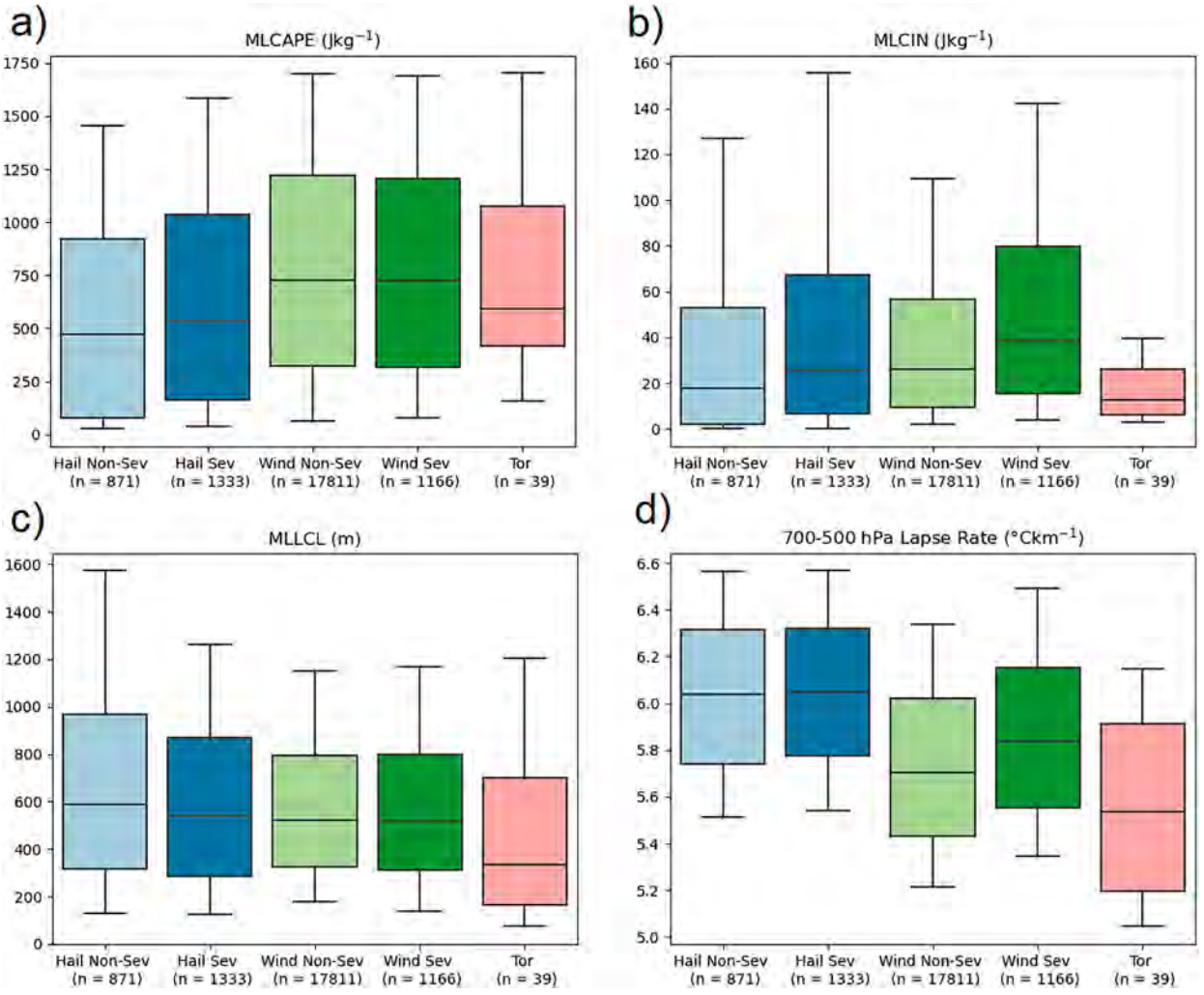

FIG. 6. Box-and-whisker plots of (a) MLCAPE, (b) MLCIN, (c) MLLCL, and (d) 700–500-hPa lapse rate. Boxes indicate the interval between 25th and 75th percentiles, and whiskers represent the 10th and 90th percentiles. The horizontal line inside the box represents the median. Convective parameters are extracted from ERA5 proximity grid points.

States for all severe weather types. These LCL heights might be associated with high boundary layer relative humidity related to the greater availability of moisture in the subtropics. For tornadoes, the median value reaches approximately 300 m, practically half of the value of those for hail and wind, agreeing with previous studies (Craven and Brooks 2004; Thompson et al. 2012) that found lower cloud base heights appear to be an important factor for tornadoes.

Severe weather events exhibit weaker midlevel lapse rates in south-central Brazil when compared to other regions (e.g., the United States and Europe; Taszarek et al. 2020). In the case of the 25th percentile for tornadoes, midlevel lapse rates are near moist adiabatic, suggesting a very different discriminant profile may be necessary compared to those developed in other regions (e.g., Brooks et al. 2003, which included lapse rate thresholds).

The results described so far represent the thermodynamic parameters distribution concerning the overall dataset. However, in an effort to capture different aspects concerning distinct CAPE regimes, the dataset has been divided into two groups: one with MLCAPE ≥ 100 J kg^{-1} (hereafter group 1) and a second with MLCAPE < 100 J kg^{-1} (hereafter group 2). Group 1 is the largest one, consisting of 18 386 pseudosoundings, of which 72% refers to the period from October to February (i.e., encompassing the peak of the Southern Hemisphere warm season). Group 2 contains 2795 pseudosoundings, 71% of them belonging to the period spanning from July to November (i.e., from midwinter to spring in the Southern Hemisphere), when stronger migratory baroclinic systems are more frequent in southern Brazil.

Consistent with the seasonal distribution described above, Fig. 7a shows that group 1 displays higher values of mean specific humidity in the lower troposphere compared to group 2. When comparing hail to wind environments, stronger moisture availability at low levels is found with the latter. As this work investigates the environments conducive to severe storms but not the storms themselves, it is not possible to address their

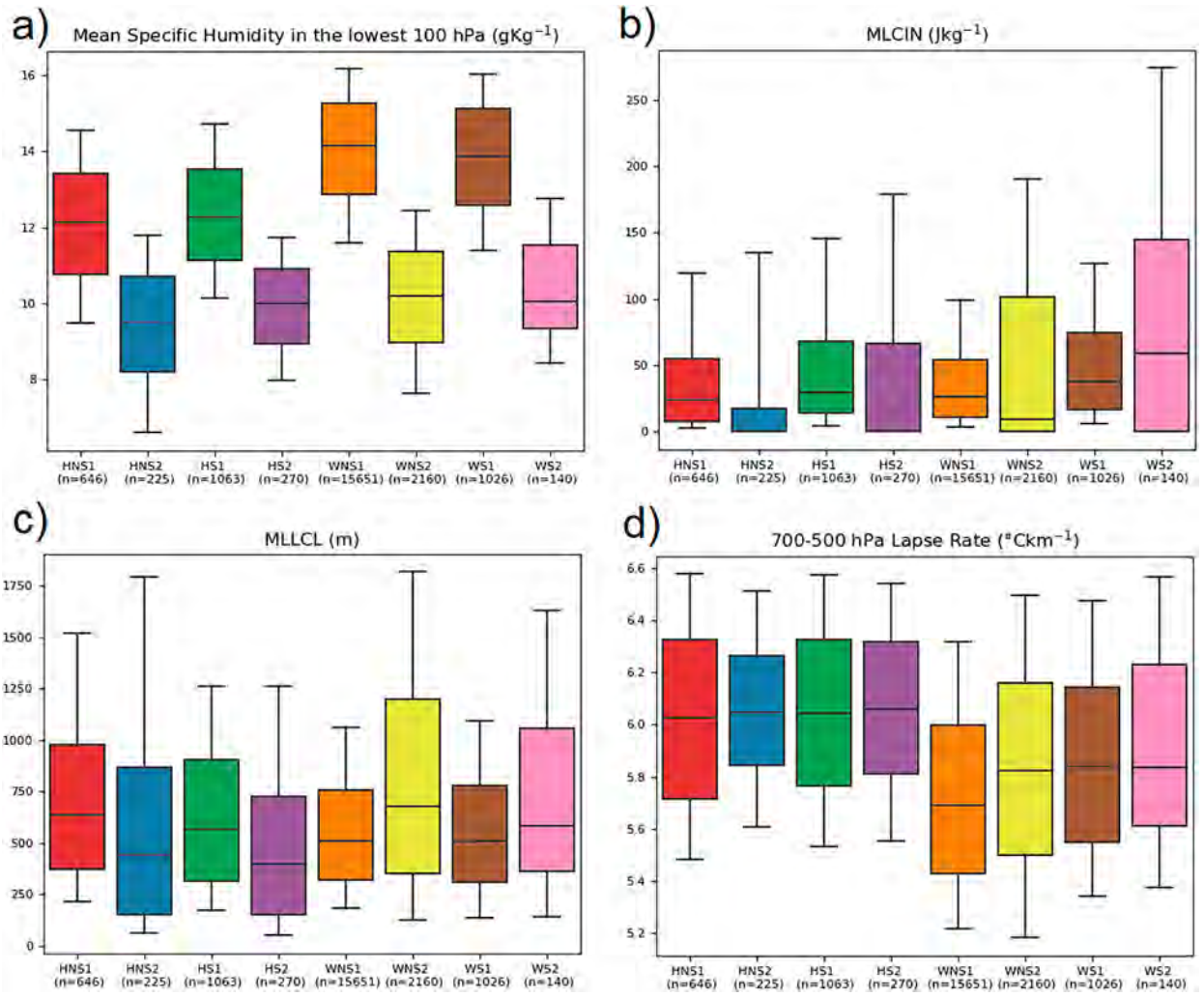

FIG. 7. As in Fig. 6, but comparing results from group 1 (MLCAPE lower than 100 J kg^{-1}) and group 2 (MLCAPE equal to or greater than 100 J kg^{-1}) and with (a) referring to the mean-specific humidity in the lowest 100 hPa. HNS = hail nonsevere; HS = hail severe; WNS = wind nonsevere; WS = wind severe; 1–group 1; 2–group 2.

microphysical properties directly. However, it is generally known that hail environments are more closely linked to the amount of moisture available in the boundary layer (Allen et al. 2015), such that air from the lowest altitudes can supply more moisture to the hail growth region of the storm (Lin and Kumjian 2022).

For wind environments, this is not necessarily true, since downdrafts can be intensified due to negatively buoyant air associated with subcloud-layer evaporation/sublimation. Otherwise, the availability of large amounts of moisture combined with high CAPE leads to a greater mass of hydrometeors that can drive strong downdrafts through contributions from the melting of hail and precipitation loading (e.g., Atlas et al. 2004).

With this in mind, as the wind environments are characterized by more moisture in the low troposphere, it is hypothesized they might be associated with wet downbursts from single or cluster cells or/and by squall lines (e.g., Ferreira and Nascimento 2016), once MCSs are favored by the low-level jet advection of warm and moist air environments in this region (Vera et al. 2006; Oliveira et al. 2018).

For the remaining parameters in Fig. 7, there is no noticeable difference concerning MLCIN and MLLCL between severe wind environments in groups 1 and 2, while LR700-500 does not separate HNS1xHNS2, HS1xHS2, and WS1xWS2, where the letter "x" in this construction means "versus" (p values > 0.05 in Table 4).

Interestingly, convective inhibition presents median (25th percentile) absolute values close to zero in group 2 hail (wind) environments, while group 1 experiences larger values for all categories. This result is consistent with the hypothesis that a fair MLCIN may delay the convective initiation until CAPE is maximized (e.g., Rasmussen and Blanchard 1998), consistent with higher values of CAPE in group 1. Moreover, the separation for this parameter is statistically significant at a 95% confidence interval for all hazard x groups, except for WS1xWS2, as already mentioned before.

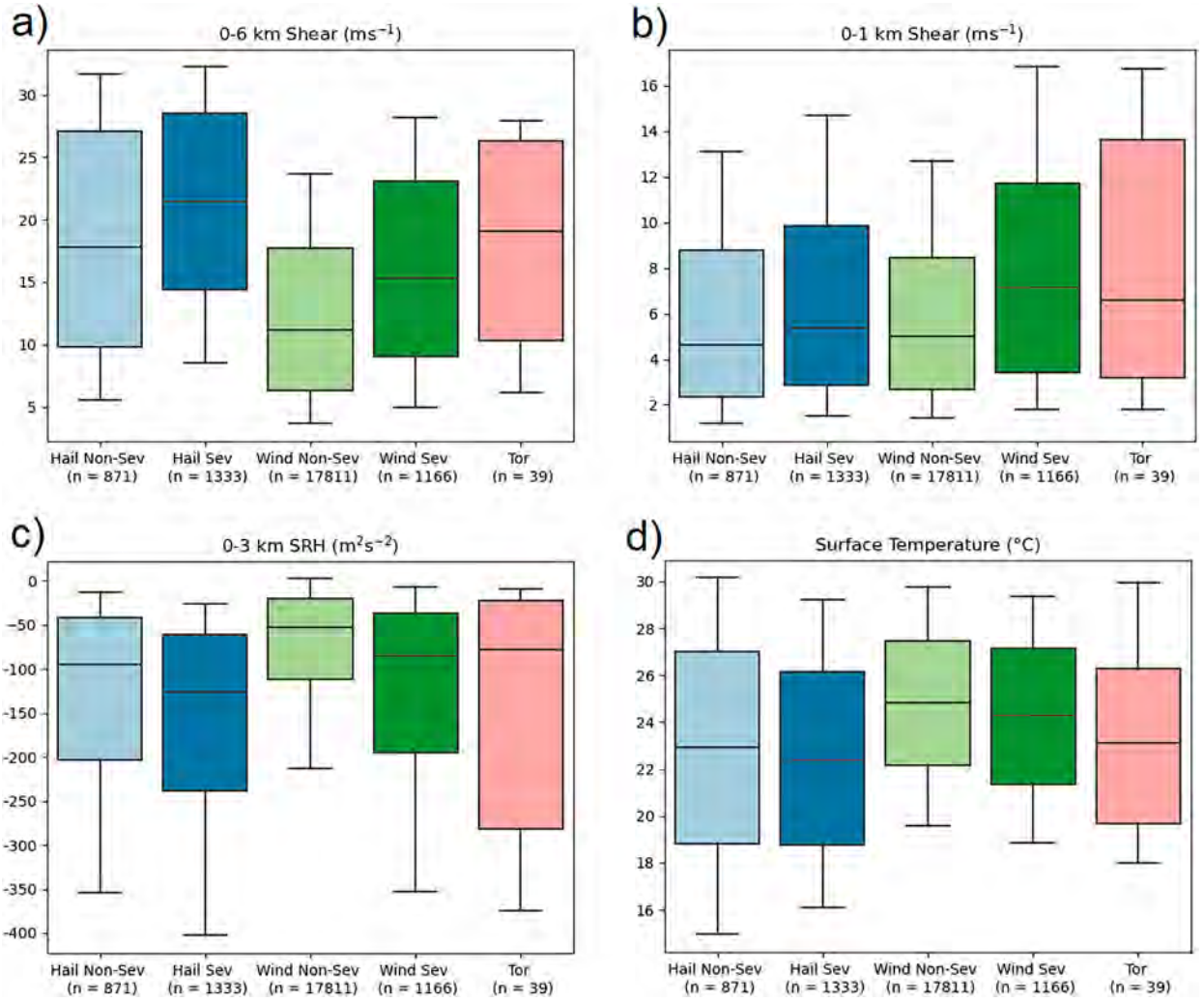

FIG. 8. As in Fig. 6, but for (a) 0–6-km bulk wind shear, (b) 0–1-km bulk wind shear, (c) 0–3-km SRH, and (d) surface temperature.

2) KINEMATIC PARAMETERS

For this study, the magnitude of the vector difference between the wind at the lowest model level and 6 km above ground level (DLS) was investigated. Results show that DLS distinguishes better between nonsevere and severe than MLCAPE for both hail and wind categories (Fig. 8a and p values in Table 4). Strong vertical wind shear has long been related to the organization of convection and associated severity (Brooks et al. 2003; Allen et al. 2011; Púčik et al. 2015; Taszarek et al. 2017). This also reflects the results of modeling studies, such as Kumjian and Lombardo (2020), who noted the relationship between high values of shear and larger sizes of hail, as intense shear leads to stronger updrafts in the hail growth area, resulting in longer hail growth trajectories. Indeed, hail stones of larger sizes (e.g., surpassing 5 cm in diameter) are often associated with supercells (Blair et al. 2017), which have their genesis intrinsically related to DLS (Thompson et al. 2012). It also is worth noticing from Fig. 8a that DLS for the hail category tends to be stronger than for the wind category when comparing their respective severe and nonsevere samples. This could be the manifestation of more diverse convective modes (beyond supercells) contributing to the sample of wind reports/observations, which is larger than the sample of hail reports.

Another relevant shear parameter is low-layer shear (LLS, 0–1-km wind shear). The values for Brazilian tornadoes (Fig. 8b) are comparable with those having a rate of F0-F1 found by Taszarek et al. (2020) over Europe, contrasting the considerably larger values found over the United States. Lopes (2020) found stronger LLS for tornadoes in southern Brazil using CFSR data, but in this specific sample, the springtime tornadoes prevailed. For hail cases, the median value for LLS does not change considerably with increasing intensity as it does for wind events (Fig. 8b and p values in Table 4), which contrasts with the increase of median values in DLS between both categories.

A useful diagnostic parameter for analyzing severe weather environments associated with organized convection is the

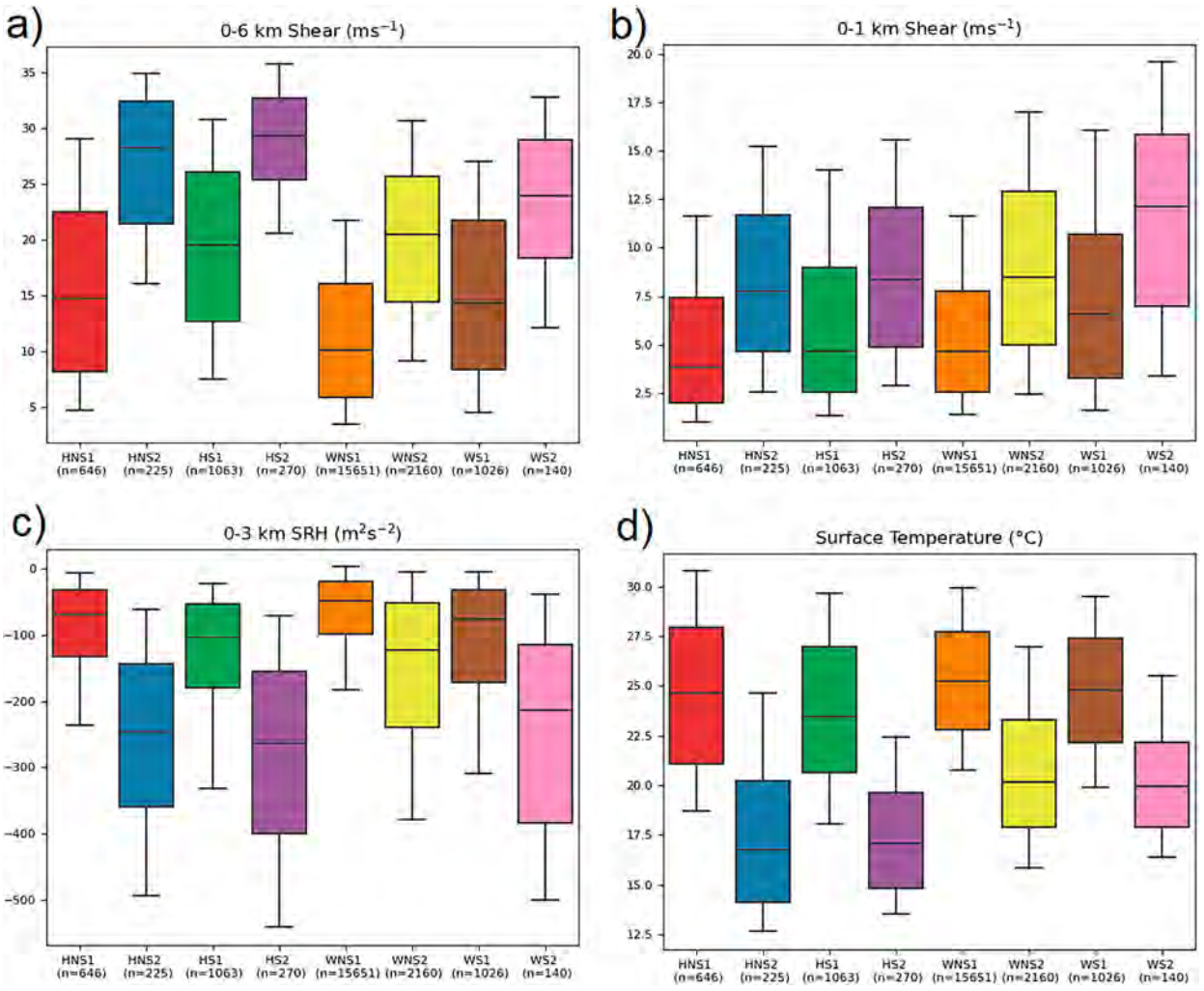

FIG. 9. As in Fig. 6, but comparing results from group 1 (MLCAPE lower than 100 J kg^{-1}) and group 2 (MLCAPE equal to or greater than 100 J kg^{-1}) for (a) 0–6-km bulk wind shear, (b) 0–1-km bulk wind shear, (c) 0–3-km SRH, and (d) surface temperature. HNS = hail nonsevere; HS = hail severe; WNS = wind nonsevere; WS = wind severe; 1–group 1; 2–group 2.

SRH. Below we analyze the relationship between the severe weather events and SRH considering the Bunkers technique applied for a left-moving cell, which is the cyclonic one in the Southern Hemisphere. One should recall that, for regimes of warm advection in the Southern Hemisphere, SRH for a left-moving storm tends to be negative (i.e., associated with antistreamwise vorticity being ingested by the updrafts for cells moving to the left of the mean wind). Despite the considerable overlap in the interquartile ranges among categories (Fig. 8c), the absolute value of SRH increases with severity in south-central Brazil; this distinction is statistically significant at the 95% level.

Evaluation of kinematic parameters in the two distinct CAPE regimes indicates considerable improvement in terms of the differences between group 1 and group 2 compared to thermodynamic parameters (p values for kinematic parameters are noticeably smaller than thermodynamic parameters in Table 4). First, the interquartile ranges for DLS present little overlap between the two groups (Fig. 9a, p value < 0.05), which means that higher DLS values tend to occur in lower CAPE environments, with the opposite occurring for higher CAPE environments. This finding also reflects the fact that in group 1 warm season pseudosoundings prevail, when strong baroclinic systems (important forcing for deep-layer vertical wind shear) are least frequent. In contrast, in group 2 a considerable portion of the sample consists of late austral winter pseudosoundings. This seasonal influence also can be assessed through the statistics of surface temperature Fig. 9d, for which the highest values are found in group 1 and the lowest in group 2, with almost no overlap between the respective interquartile ranges (Fig. 9d, p value < 0.05). Another important result is that the separation between groups 1 and 2 does not change the general tendency for DLS to be stronger for the hail category than for the wind category when their respective severe and nonsevere samples are compared (Fig. 9a).

In terms of LLS (Fig. 9b), the overlap of interquartile ranges between groups 1 and 2 is reduced when compared to

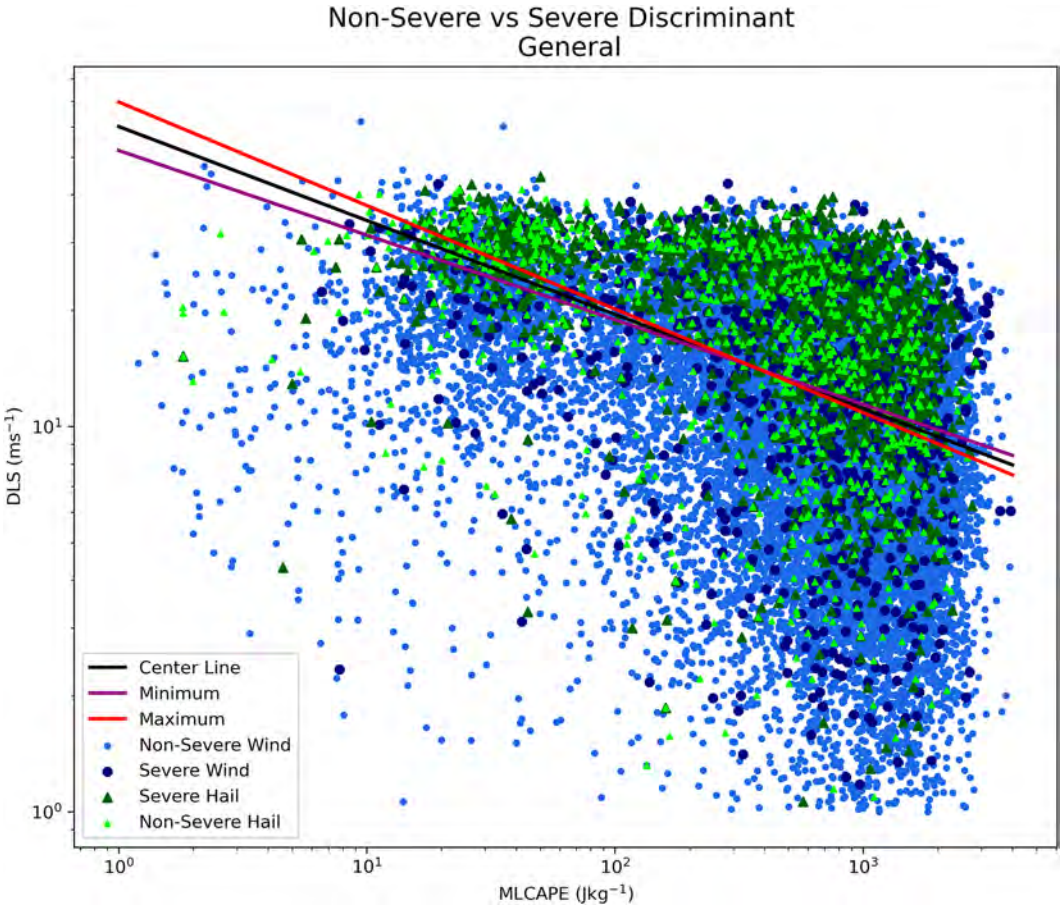

FIG. 10. Distribution of proximity pseudosoundings for nonsevere (light green triangle for hail and blue circle for wind) and severe (green triangle for hail and dark blue for wind) in log-CAPE–log-DLS phase space. The center line corresponds to the discriminant determined for all proximity soundings [Eq. (2), line denoted in black] with the minimum and maximum discriminant lines (purple and red, respectively) determined by $\text{CAPE} \times \text{DLS}^{4.55} \geq 64\,858\,337$ and $\text{CAPE} \times \text{DLS}^{3.72} \geq 7\,166\,910$.

the respective overlaps found between the distinct hail and wind samples belonging to the same group (i.e., to the same CAPE regime), in agreement with their respective p values < 0.05 (Table 4). Clearly, LLS in group 2 is stronger than in group 1. To some extent, these higher values of LLS in lower CAPE environments may be related to the more frequent presence of the low-level jet in the austral winter and spring in southern Brazil (Oliveira et al. 2018).

The variability of SRH3 in group 2 environments is higher than in group 1 (Fig. 9c), with SRH3 also displaying more negative values in group 2. Combined with the result discussed for DLS and LLS, this finding indicates that, under a low CAPE regime (group 2), the kinematic parameters play an even more important role in characterizing the convective environment. It should be no surprise that group 2 displays such behavior because, in relative terms, it is the sample

TABLE 5. Skill scores for discriminant functions determined using the PREVOTS and DECEA+INMET proximity database, with variations in the convective weather threat and MLCAPE regime.

Discriminant	Shear exponent	Threshold	Accuracy	POD	POFD	CSI	HSS
General	4.10	19 691 164	0.602 ± 0.0079	0.611 ± 0.0056	0.404 ± 0.0195	0.426 ± 0.0240	0.205 ± 0.0150
Hail	2.92	224 847	0.634 ± 0.0247	0.596 ± 0.0386	0.352 ± 0.0019	0.282 ± 0.0074	0.194 ± 0.0170
Wind	4.34	21 249 148	0.616 ± 0.0139	0.613 ± 0.0051	0.381 ± 0.0915	0.465 ± 0.0074	0.239 ± 0.006
MLCAPE $\geq$ 100 J kg^{-1}	3.88	13 355 291	0.648 ± 0.0197	0.628 ± 0.0246	0.328 ± 0.0151	0.492 ± 0.0295	0.298 ± 0.0385
MLCAPE $<$ 100 J kg^{-1}	3.16	676 592	0.604 ± 0.0254	0.587 ± 0.0022	0.380 ± 0.0299	0.413 ± 0.0519	0.204 ± 0.0527

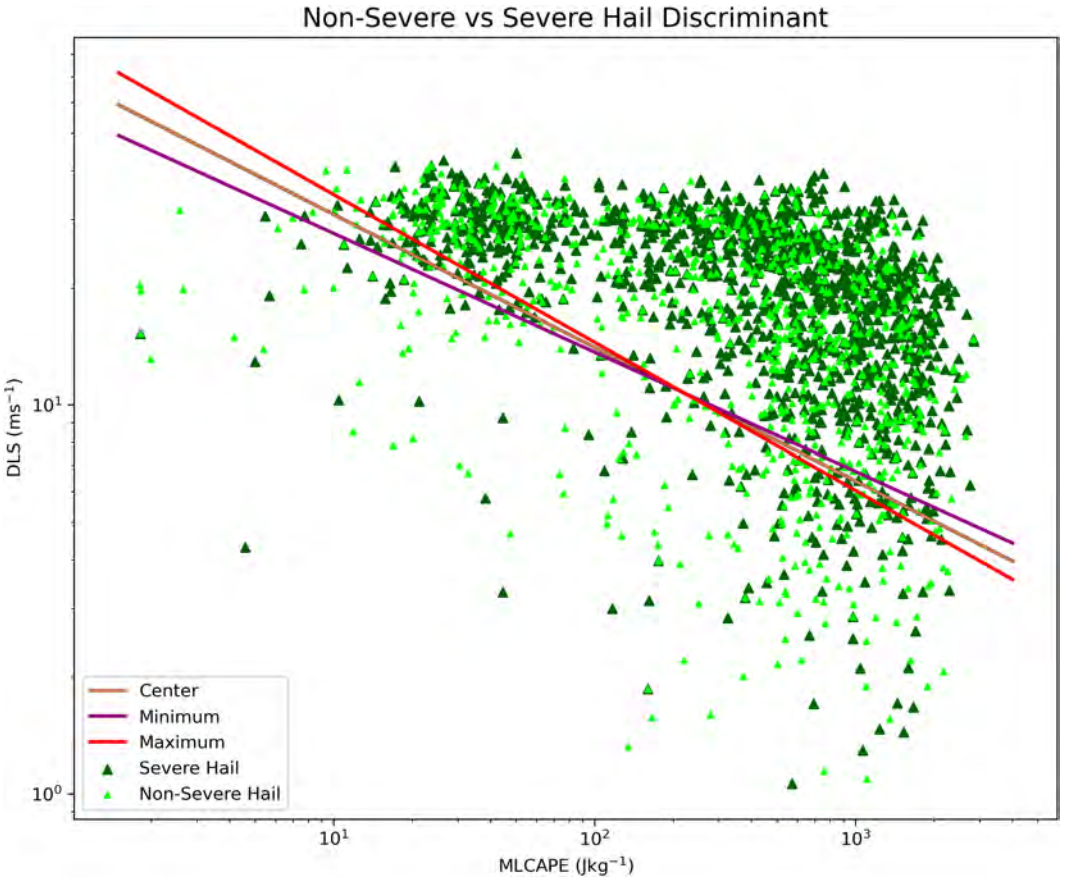

FIG. 11. Distribution of proximity pseudosoundings for nonsevere (light green triangle) and severe (green triangle) in log-CAPE–log-DLS phase space only for hail proximity soundings. The center line corresponds to the discriminant determined (CAPE $\times$ DLS$^{2.92} \geq 224\,847$, line denoted in brown) with the minimum and maximum discriminant lines (purple and red, respectively) determined by CAPE $\times$ DLS$^{3.27} \geq 517\,606$ and CAPE $\times$ DLS$^{2.63} \geq 113\,353$.

containing more proximity pseudosoundings associated with the cold season, typical of low-CAPE high-shear environments.

d. Brazilian severe storm discriminants

A linear discriminant analysis was performed using the subset of proximity soundings to PREVOTS convective storm reports and to DECEA+INMET convectively induced wind gusts in order to find an appropriate combination of CAPE and wind shear that can discriminate between environments of nonsevere and severe storms.

The general discriminant for Brazilian severe storm events found to be defined by the function:

$$0.4591 \log(\text{CAPE}) + 1.8822 \log(\text{DLS}) \geq 3.3488, \quad (1)$$

which simplifies to

$$\text{CAPE} \times \text{DLS}^{4.10} \geq 19\,691\,164. \quad (2)$$

The general linear discriminant and a slope of minimum and maximum angle from the set of discriminants determined are shown in Fig. 10. The discriminant method relying on the centroid of the set of points meant that the three lines pass through a common point (black line in Fig. 10). Above this line, soundings are more likely to be related to severe storms. Note that the aforementioned discriminant was developed including reports for both hail and wind.

To assess how the specific hazards and MLCAPE regimes were driving the general discriminant performance, consistent with the recommendations of Brooks (2013), four additional fitted relationships were explored. The first considers only hail events, the second uses only wind reports, the third uses only reports associated with MLCAPE ≥ 100 J kg^{-1} (group 1), and the fourth with only reports related to MLCAPE < 100 J kg^{-1} (group 2). Their respective shear exponents and thresholds are shown in Table 5, in addition to their skill scores.

Considering the skill scores for the different categories, the best performance is for group 1 (MLCAPE ≥ 100 J kg^{-1}) with the best scores for all parameters. The discriminant for nonsevere and severe wind also shows a suitable performance according to its skill scores. On the other hand, it is not possible to affirm that one specific type has the worst performance, once the scores vary their efficiency throughout the remaining categories. This result is possibly related to the sample size, as

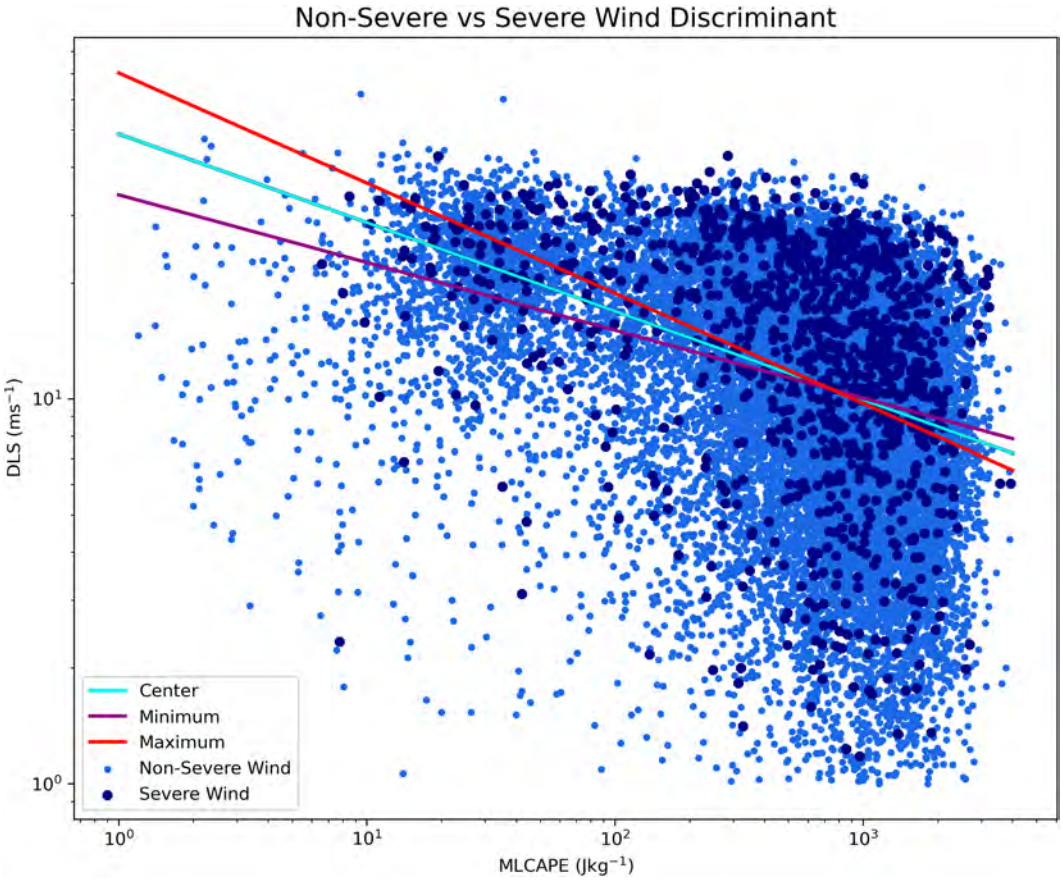

FIG. 12. Distribution of proximity pseudosoundings for nonsevere (blue circle) and severe (dark blue circle) in log-CAPE–log-DLS phase space only for wind proximity soundings. The center line corresponds to the discriminant determined (CAPE $\times$ DLS$^{4.34} \geq 21\,249\,148$, line denoted in light blue) with the minimum and maximum discriminant lines (purple and red, respectively) determined by CAPE $\times$ DLS$^{5.68} \geq 490\,846\,472$ and CAPE $\times$ DLS$^{3.49} \geq 2\,799\,773$.

wind and MLCAPE ≥ 100 J kg^{-1} represent the largest contribution to the database. In turn, the model has more possibilities to fit/learn on the training dataset in order to optimize a predefined loss function (Chase et al. 2022).

Figures 11 and 12 show the graphical depiction of wind and hail samples and their respective discriminants separately, as opposed to including all cases within a single figure. This approach enables us to observe how heavily the entire sample relies on wind reports, as discussed in section 2e. In addition, it is important to note that the distance between minimum and maximum discriminants is smaller in the hail sample (Fig. 11), whereas discriminants for wind (Fig. 12) show more variability.

The line slope representing the discrimination in MLCAPE ≥ 100 J kg^{-1} (group1, pink line in Figs. 13a and 14) is the closest to the general fitted relationship. This is unsurprising given that the largest part of the proximity-soundings sample (approximately 87%) is composed of environments with MLCAPE greater than 100 J kg^{-1}. The discriminant for group 1 also presents the lowest POFD (probability of false detection), which means that a smaller fraction of observed nonsevere cases were considered severe by the model when compared to the other discriminants.

In Fig. 14, previous discriminants produced for the United States for significant severe to severe (Brooks et al. 2003) and for Australia (Allen et al. 2011; Allen and Karoly 2014) are shown for comparison. The primary difference between Brazilian cases and both the U.S. and Australian environments is the presence of more high-shear and low CAPE cases in Brazil. This does not necessarily mean these two other regions do not experience environments with low CAPE associated with severe weather (e.g., Sherburn and Parker 2014), but it is probably a consequence of the choice to cut off the proximity sounding MLCAPE at 100 J kg^{-1} in previous work, while the present work considers any MLCAPE value greater than 1 J kg^{-1}.

Furthermore, DLS plays a greater role in Brazil's severe storm environments, which can be demonstrated by a higher exponent "weighting" the shear parameter (4.10 in contrast to 1.6 in the United States and 1.67 in Australia). It should also be noted that the severe parameter developed by Allen and Karoly (2014) was only estimated, as no record of subsevere events was available to fit this relationship as we have here. In

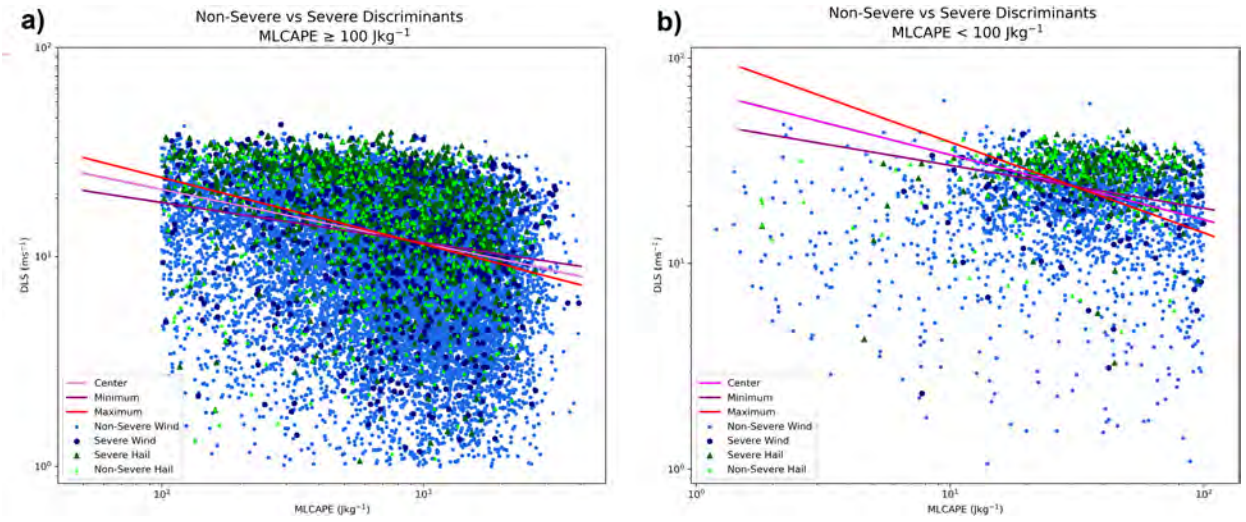

FIG. 13. (a) South-central Brazilian's discriminants for MLCAPE $\geq$ 100 J kg^{-1} environments; the center line is denoted in pink (CAPE $\times$ DLS$^{3.88}$ $\geq$ 13 355 291), with the minimum and maximum discriminant lines (purple and red, respectively) determined by CAPE $\times$ DLS$^{5.22}$ $\geq$ 404 341 467 and CAPE $\times$ DLS$^{3.14}$ $\geq$ 2 122 233. (b) As in (a), but for MLCAPE $<$ 100 J kg^{-1} environments; the center line is denoted in light pink (CAPE $\times$ DLS$^{3.16}$ $\geq$ 676 592), with the minimum and maximum discriminant lines (purple and red, respectively) determined by CAPE $\times$ DLS$^{4.77}$ $\geq$ 111 479 456 and CAPE $\times$ DLS$^{2.26}$ $\geq$ 34 377.

prior evaluation of climatological frequency, the thresholds established for the U.S. and Australia severe storm environments have been found to be too low for Brazilian cases (46 800 and 68 000 compared to 19 691 164), which may also be related to the overall greater exponent value in DLS, despite lower CAPE values.

For the application of these discriminants as proxies for climatological concerns, some caution should be taken to represent each group's particularity. As all discriminants present an important "weight" on the shear parameter, if a minimum cutoff for CAPE is not considered, regional biases on the severe weather environments may occur in higher latitudes due to a greater shear magnitude (e.g., during winter and spring, following the climatological position of the upper-level jet stream–baroclinicity). MLCAPE $\geq$ 100 J kg^{-1} discriminant could be a reasonable choice in this situation. Despite the importance given to shear within all discriminants, severe hail discriminant has the lowest shear exponent, suggesting that environments conducive to severe hail events differ from those found to compose severe wind environments, at least in terms of CAPE and shear. Applying minimum cutoff values for both CAPE and shear for severe hail and severe wind discriminants should properly calibrate each environment singularity.

SENSITIVITY TO THE PROXIMITY TIME CHOICE

The parameters employed to describe the different discriminants in the previous subsection were computed from ERA5 tropospheric profiles nearest to the hail and wind reports/observations in both space and time. This raises the possibility of some profiles being influenced by ongoing convection (e.g., "convectively contaminated"). In a contaminated profile CAPE is reduced due to the consumption of convective energy by the storms in progress such that the notion of a preconvective environment (associated with proximity soundings) is not met. It is natural to expect that profiles preceding (subsequent to) the time of the weather reports/observations are the ones least (more) likely to be contaminated by convection.

In an effort to assess the sensitivity of the discriminant analysis to the time criterion utilized to obtain the ERA5 profiles, we have computed a new set of discriminants based on the choice of always selecting such profiles from the closest hour *preceding* the weather event for each category (Table 6). We are aware that it does not guarantee these new set of environments will not be convectively contaminated, but it provides an opportunity to, at least, assess the sensibility of the proximity-sounding time choice.

Except for MLCAPE $<$ 100 discriminant, all the others present a reduction in the shear exponent, suggesting a greater role of the CAPE parameter in "preconvective" environments compared to the "closest" environments, as expected.

For the general, wind, and MLCAPE $\geq$ 100 discriminants, the threshold was reduced in one magnitude order, while the hail discriminant remained with the same magnitude order. Interestingly, MLCAPE $<$ 100 discriminant for preconvective environments displays an increase in three magnitude orders in the threshold (together with a substantial increase in the shear exponent), implying an even more important shear role, in detriment of CAPE.

Skill scores remain virtually the same in the general discriminants (cf. Tables 5 and 6), and display an overall improved performance in the closest environments for wind and MLCAPE $\geq$ 100. Concerning the skill scores for hail and MLCAPE $<$ 100 discriminants, some are better for preconvective environments (e.g., POD in hail discriminant), others for the closest environments (e.g., CSI for MLCAPE $<$ 100 discriminant), suggesting no definitive conclusion about which one presents the best choice.

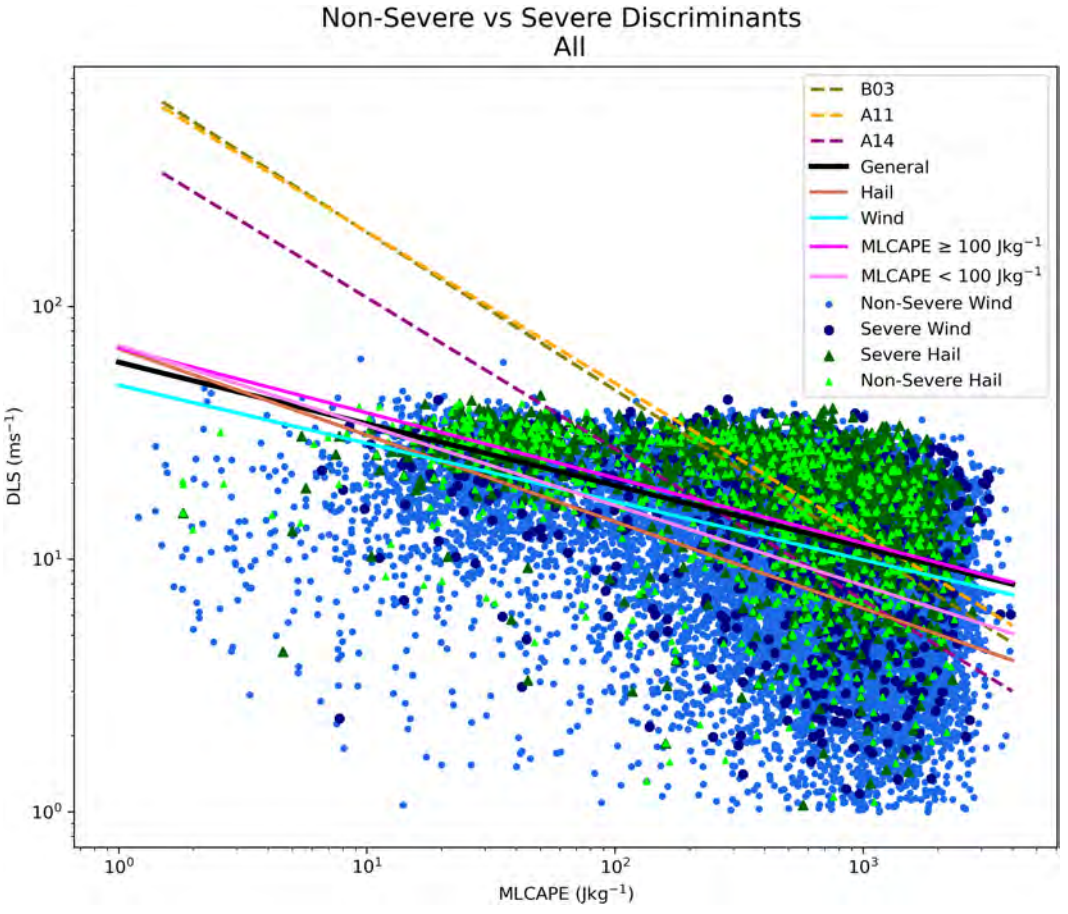

FIG. 14. South-central Brazilian's discriminants for the present general discriminant (black line), hail discriminant (brown line), wind discriminant (light blue line), MLCAPE $\geq$ 100 J kg^{-1} environments discriminant (pink line), and MLCAPE $<$ 100 J kg^{-1} (light pink line). Also shown are the original Brooks et al. (2003) significant severe/severe discriminant (olive dashed line), the Allen et al. (2011) significant severe/severe discriminant (orange dashed line), and the Allen and Karoly (2014) severe/nonsevere discriminant estimate (purple dashed line).

4. Summary and conclusions

Based on two databases in south-central Brazil, different nonsevere to severe storm discriminants were produced using ERA5 pseudoproximity soundings. This article has been the first to develop such a discriminant analysis for Brazilian severe weather environments. The discriminants performed here do provide an important improvement concerning the understanding of the unique regional characteristics of the severe weather environments in this region.

The monthly distribution of severe weather in south-central Brazil demonstrates the highest frequency of occurrence between spring and summer and the lowest in autumn. Diurnally, the highest frequency is found in the midafternoon and a weaker peak is observed during nocturnal hours. These extended nocturnal hours have been previously identified by (Bruick et al. 2019) for hailstorms in subtropical South America, but it differs from what is observed in the United States (Allen and Tippett 2015).

TABLE 6. Skill scores for discriminant functions determined using the PREVOTS and DECEA+INMET one hour before the proximity database, with variations in the convective weather threat and MLCAPE regime.

Discriminant	Shear exponent	Threshold	Accuracy	POD	POFD	CSI	HSS
General	3.63	5 985 706	0.605 ± 0.0188	0.606 ± 0.0417	0.396 ± 0.0024	0.425 ± 0.0308	0.210 ± 0.0390
Hail	2.54	386 561	0.570 ± 0.0029	0.638 ± 0.0458	0.469 ± 0.0224	0.382 ± 0.0348	0.156 ± 0.0100
Wind	3.65	3 834 250	0.580 ± 0.0356	0.596 ± 0.0448	0.435 ± 0.0268	0.427 ± 0.0301	0.161 ± 0.0718
MLCAPE $\geq$ 100 J kg^{-1}	3.61	2 622 569	0.630 ± 0.0051	0.624 ± 0.0176	0.376 ± 0.0175	0.352 ± 0.1236	0.207 ± 0.0412
MLCAPE $<$ 100 J kg^{-1}	5.27	129 250 463	0.609 ± 0.0238	0.707 ± 0.0037	0.450 ± 0.0558	0.392 ± 0.0584	0.254 ± 0.0056

Overall, DLS distinguishes better between nonsevere and severe than MLCAPE, with p values for kinematic parameters noticeably smaller than thermodynamic parameters among the categories, indicating a stronger statistical significance. When the two distinct CAPE regimes are examined, DLS presents almost no overlap between the two groups of CAPE, with higher DLS values mostly occurring in lower CAPE environments and conversely for higher CAPE environments. Furthermore, surface temperature depicts statistically significant values at the 95% confidence interval between group 1 and group 2 as well, and is clearly divided between them, suggesting a surface temperature/seasonal dependence for the two different CAPE regimes.

As for the linear discriminants, the best performance is detected for group 1 (MLCAPE $\geq$ 100 J kg^{-1}) with the best scores for all parameters. The discriminant for nonsevere and severe wind also shows a suitable performance according to its skill scores.

Compared with previous discriminants produced for the United States and Australia, the primary difference for Brazilian environment cases is the presence of more high-shear and low-CAPE cases in Brazil. Another peculiarity is DLS plays a greater role in Brazil's severe storm environments, which can be demonstrated by a higher exponent "weighting" the shear parameter. This indicates that prior discriminants were not sufficient to characterize observed severe convective environments in south-central Brazil.

Future work will include an application of these discriminants to determine the evolution of severe storm environments over subtropical South America in the last decades, trends of these environments, possible factors affecting their interannual variability, and how they will possibly change under different climate change scenarios for this region.

Acknowledgments. This research was supported by grants from the Coordenação de Aperfeiçoamento de Pessoal de Nível Superior and Fulbright Program. J. Allen's contribution was supported by the National Science Foundation under Grant AGS-1945286. The authors are grateful to the three anonymous reviewers for their comments that improved the manuscript. We also thank Leornardo Furlan for the quality-controlled soundings, and Vanessa Ferreira, Matthew Vallis, and the PREVOTS team for their support with the data utilized in this study.

Data availability statement. ERA5 data (temperature, specific humidity, pressure, and u and v winds) were downloaded from the European Centre for Medium-Range Weather Forecasts (ECMWF), Copernicus Climate Change Service (C3S) at Climate Data Store (https://cds.climate.copernicus.eu/). Brazil severe weather reports are from Plataforma de Registros e Rede Voluntária de Observadores de Tempo Severo (PREVOTS) and due to the proprietary nature of the data, cannot be made openly available, contact prevots.svr@gmail.com for usage information.

REFERENCES

Allen, J. T., and D. J. Karoly, 2014: A climatology of Australian severe thunderstorm environments 1979–2011: Inter-annual variability and ENSO influence. *Int. J. Climatol.*, **34**, 81–97, https://doi.org/10.1002/joc.3667.

——, and M. K. Tippett, 2015: The characteristics of the United States hail reports: 1955–2014. *Electron. J. Severe Storms Meteor.*, **10** (3), https://ejssm.com/ojs/index.php/site/article/view/60.

——, D. J. Karoly, and G. A. Mills, 2011: A severe thunderstorm climatology for Australia and associated thunderstorm environments. *Aust. Meteor. Oceanogr. J.*, **61**, 143–158, https://doi.org/10.22499/2.6103.001.

——, M. K. Tippett, and A. H. Sobel, 2015: An empirical model relating U.S. monthly hail occurrence to large-scale meteorological environment. *J. Adv. Model. Earth Syst.*, **7**, 226–243, https://doi.org/10.1002/2014MS000397.

——, E. R. Allen, H. Richter, and C. Lepore, 2021: Australian tornadoes in 2013: Implications for climatology and forecasting. *Mon. Wea. Rev.*, **149**, 1211–1232, https://doi.org/10.1175/MWR-D-20-0248.1.

Anabor, V., D. J. Stensrud, and O. L. L. de Moraes, 2008: Serial upstream-propagating mesoscale convective system events over southeastern South America. *Mon. Wea. Rev.*, **136**, 3087–3105, https://doi.org/10.1175/2007MWR2334.1.

Atlas, D., C. W. Ulbrich, and C. R. Williams, 2004: Physical origin of a wet microburst: Observations and theory. *J. Atmos. Sci.*, **61**, 1186–1195, https://doi.org/10.1175/1520-0469(2004)061<1186:POOAWM>2.0.CO;2.

Beal, A., R. Hallak, L. D. Martins, J. A. Martins, G. Biz, A. P. Rudke, and C. R. T. Tarley, 2020: Climatology of hail in the triple border Paraná, Santa Catarina (Brazil) and Argentina. *Atmos. Res.*, **234**, 104747, https://doi.org/10.1016/j.atmosres.2019.104747.

Bechis, H., and Coauthors, 2022: A case study of a severe hailstorm in Mendoza, Argentina, during the RELAMPAGO-CACTI field campaign. *Atmos. Res.*, **271**, 106127, https://doi.org/10.1016/j.atmosres.2022.106127.

Bender, A., E. D. Freitas, and L. A. T. Machado, 2019: The impact of future urban scenarios on a severe weather case in the metropolitan area of São Paulo. *Climatic Change*, **156**, 471–488, https://doi.org/10.1007/s10584-019-02527-1.

Blair, S. F., and Coauthors, 2017: High-resolution hail observations: Implications for NWS warning operations. *Wea. Forecasting*, **32**, 1101–1119, https://doi.org/10.1175/WAF-D-16-0203.1.

Blamey, R. C., C. Middleton, C. Lennard, and C. J. C. Reason, 2017: A climatology of potential severe convective environments across South Africa. *Climate Dyn.*, **49**, 2161–2178, https://doi.org/10.1007/s00382-016-3434-7.

Borque, P., L. Vidal, M. Rugna, T. J. Lang, M. G. Nicora, and S. W. Nesbitt, 2020: Distinctive signals in 1-min observations of overshooting tops and lightning activity in a severe supercell thunderstorm. *J. Geophys. Res. Atmos.*, **125**, e2020JD032856, https://doi.org/10.1029/2020JD032856.

Brooks, H. E., 2013: Severe thunderstorms and climate change. *Atmos. Res.*, **123**, 129–138, https://doi.org/10.1016/j.atmosres.2012.04.002.

——, J. W. Lee, and J. P. Craven, 2003: The spatial distribution of severe thunderstorm and tornado environments from global reanalysis data. *Atmos. Res.*, **67–68**, 73–94, https://doi.org/10.1016/S0169-8095(03)00045-0.

——, A. R. Anderson, K. Riemann, I. Ebbers, and H. Flachs, 2007: Climatological aspects of convective parameters from the NCAR/NCEP reanalysis. *Atmos. Res.*, **83**, 294–305, https://doi.org/10.1016/j.atmosres.2005.08.005.

Bruick, Z. S., K. L. Rasmussen, and D. J. Cecil, 2019: Subtropical South American hailstorm characteristics and environments.

Mon. Wea. Rev., **147**, 4289–4304, https://doi.org/10.1175/MWR-D-19-0011.1.

Bunkers, M. J., B. A. Klimowski, J. W. Zeitler, R. L. Thompson, and M. L. Weisman, 2000: Predicting supercell motion using a new hodograph technique. *Wea. Forecasting*, **15**, 61–79, https://doi.org/10.1175/1520-0434(2000)015<0061:PSMUAN>2.0.CO;2.

Cecil, D. J., and C. B. Blankenship, 2012: Toward a global climatology of severe hailstorms as estimated by satellite passive microwave imagers. *J. Climate*, **25**, 687–703, https://doi.org/10.1175/JCLI-D-11-00130.1.

Chase, R. J., D. R. Harrison, A. Burke, G. M. Lackmann, and A. McGovern, 2022: A machine learning tutorial for operational meteorology. Part I: Traditional machine learning. *Wea. Forecasting*, **37**, 1509–1529, https://doi.org/10.1175/WAF-D-22-0070.1.

Coffer, B. E., M. Taszarek, and M. D. Parker, 2020: Near-ground wind profiles of tornadic and nontornadic environments in the United States and Europe from ERA5 reanalyses. *Wea. Forecasting*, **35**, 2621–2638, https://doi.org/10.1175/WAF-D-20-0153.1.

Coniglio, M. C., and M. D. Parker, 2020: Insights into supercells and their environments from three decades of targeted radiosonde observations. *Mon. Wea. Rev.*, **148**, 4893–4915, https://doi.org/10.1175/MWR-D-20-0105.1.

——, and R. E. Jewell, 2022: SPC mesoscale analysis compared to field-project soundings: Implications for supercell environment studies. *Mon. Wea. Rev.*, **150**, 567–588, https://doi.org/10.1175/MWR-D-21-0222.1.

Craven, J. P., and H. E. Brooks, 2004: Baseline climatology of sounding derived parameters associated with deep moist convection. *Natl. Wea. Dig.*, **28**, 13–24.

Doswell, C. A., III, and D. M. Schultz, 2006: On the use of indices and parameters in forecasting severe storms. *Electron. J. Severe Storms Meteor.*, **1** (3), https://ejssm.org/archives/wp-content/uploads/2021/09/vol1-3.pdf.

——, H. E. Brooks, and R. A. Maddox, 1996: Flash-flood forecasting: An ingredients-based methodology. *Wea. Forecasting*, **11**, 560–581, https://doi.org/10.1175/1520-0434(1996)011<0560:FFFAIB>2.0.CO;2.

EMATER/ASCAR, 2021: Laudo técnico dos prejuízos decorrentes de chuva de granizo no município de Bom Jesus—RS (in Portuguese). EMATER/ASCAR, 2 pp.

Ferreira, V., and E. L. Nascimento, 2016: Convectively-induced severe wind gusts in southern Brazil: Surface observations, atmospheric environment, and association with distinct convective modes. *28th Conf. on Severe Local Storms*, Portland, OR, Amer. Meteor. Soc., 142, https://ams.confex.com/ams/28SLS/webprogram/Paper299442.html.

——, V. Goede, and E. L. Nascimento, 2022: An environmental and polarimetric study of the 19 November 2015 supercell and multiple-vortex tornado in Marechal Cândido Rondon, southern Brazil. *Meteor. Atmos. Phys.*, **134**, 82, https://doi.org/10.1007/s00703-022-00922-5.

Figueiredo, E., E. Nascimento, and M. I. Oliveira, 2019: Analysis of two derecho events in southern Brazil. *Meteor. Atmos. Phys.*, **131**, 1171–1190, https://doi.org/10.1007/s00703-018-0654-x.

Gensini, V. A., and W. S. Ashley, 2011: Climatology of potentially severe convective environments from the North American regional reanalysis. *Electron. J. Severe Storms Meteor.*, **6** (8), https://ejssm.org/archives/wp-content/uploads/2021/09/vol6-8.pdf.

——, and H. E. Brooks, 2018: Spatial trends in United States tornado frequency. *npj Climate Atmos. Sci*, **1**, 38,https://doi.org/10.1038/s41612-018-0048-2.

——, T. L. Mote, and H. E. Brooks, 2014: Severe-thunderstorm reanalysis environments and collocated radiosonde observations. *J. Appl. Meteor. Climatol.*, **53**, 742–751, https://doi.org/10.1175/JAMC-D-13-0263.1.

Glazer, R. H., J. A. Torres-Alavez, E. Coppola, F. Giorgi, S. Das, M. Ashfaq, and T. Sines, 2021: Projected changes to severe thunderstorm environments as a result of twenty-first century warming from RegCM CORDEX-CORE simulations. *Climate Dyn.*, **57**, 1595–1613, https://doi.org/10.1007/s00382-020-05439-4.

Hersbach, H., and Coauthors, 2020: The ERA5 global reanalysis. *Quart. J. Roy. Meteor. Soc.*, **146**, 1999–2049, https://doi.org/10.1002/qj.3803.

Kumjian, M. R., and K. Lombardo, 2020: A hail growth trajectory model for exploring the environmental controls on hail size: Model physics and idealized tests. *J. Atmos. Sci.*, **77**, 2765–2791, https://doi.org/10.1175/JAS-D-20-0016.1.

Lagerquist, R., A. McGovern, and T. Smith, 2017: Machine learning for real-time prediction of damaging straight-line convective wind. *Wea. Forecasting*, **32**, 2175–2193, https://doi.org/10.1175/WAF-D-17-0038.1.

Lepore, C., R. Abernathey, N. Henderson, J. T. Allen, and M. K. Tippett, 2021: Future global convective environments in CMIP6 models. *Earth's Future*, **9**, e2021EF002277, https://doi.org/10.1029/2021EF002277.

Li, F., D. R. Chavas, K. A. Reed, and D. T. Dawson II, 2020: Climatology of severe local storm environments and synoptic-scale features over North America in ERA5 reanalysis and CAM6 simulation. *J. Climate*, **33**, 8339–8365, https://doi.org/10.1175/JCLI-D-19-0986.1.

Li, M., D.-L. Zhang, J. Sun, and Q. Zhang, 2018: A statistical analysis of hail events and their environmental conditions in China during 2008–15. *J. Appl. Meteor. Climatol.*, **57**, 2817–2833, https://doi.org/10.1175/JAMC-D-18-0109.1.

Lin, Y., and M. R. Kumjian, 2022: Influences of CAPE on hail production in simulated supercell storms. *J. Atmos. Sci.*, **79**, 179–204, https://doi.org/10.1175/JAS-D-21-0054.1.

Lopes, M., 2020: Discriminando condições favoráveis a diferentes modos de tempo severo no leste da bacia do prata. M.S. thesis, Universidade Federal de Santa Maria, 122 pp.

Martins, J. A., and Coauthors, 2017: Climatology of destructive hailstorms in Brazil. *Atmos. Res.*, **184**, 126–138, https://doi.org/10.1016/j.atmosres.2016.10.012.

Matsudo, C. M., and P. V. Salio, 2011: Severe weather reports and proximity to deep convection over northern Argentina. *Atmos. Res.*, **100**, 523–537, https://doi.org/10.1016/j.atmosres.2010.11.004.

Mulholland, J. P., S. W. Nesbitt, R. J. Trapp, K. L. Rasmussen, and P. V. Salio, 2018: Convective storm life cycle and environments near the Sierras de Córdoba, Argentina. *Mon. Wea. Rev.*, **146**, 2541–2557, https://doi.org/10.1175/MWR-D-18-0081.1.

——, ——, ——, and J. M. Peters, 2020: The influence of terrain on the convective environment and associated convective morphology from an idealized modeling perspective. *J. Atmos. Sci.*, **77**, 3929–3949, https://doi.org/10.1175/JAS-D-19-0190.1.

Nascimento, E. L., G. Held, and A. M. Gomes, 2014: A multiple vortex tornado in southeastern Brazil. *Mon. Wea. Rev.*, **142**, 3017–3037, https://doi.org/10.1175/MWR-D-13-00319.1.

——, M. Foss, V. Ferreira, and H. E. Brooks, 2016: An updated and expanded climatology of severe weather parameters for subtropical South America as derived from upper air observations and CFSR-CFSV2 data. *28th Conf. on Severe Local Storms*, Portland, OR, Amer. Meteor. Soc., 18.5, https://ams.confex.com/ams/28SLS/webprogram/Paper300887.html.

Nesbitt, S. W., and Coauthors, 2021: A storm safari in subtropical South America: Proyecto RELAMPAGO. *Bull. Amer. Meteor. Soc.*, **102**, E1621–E1644, https://doi.org/10.1175/BAMS-D-20-0029.1.

Oliveira, M. I., E. L. Nascimento, and C. Kannenberg, 2018: A new look at the identification of low-level jets in South America. *Mon. Wea. Rev.*, **146**, 2315–2334, https://doi.org/10.1175/MWR-D-17-0237.1.

——, F. S. Puhales, E. L. Nascimento, and V. Anabor, 2022: Integrated damage, visual, remote sensing, and environmental analysis of a strong tornado in southern Brazil. *Atmos. Res.*, **274**, 106188, https://doi.org/10.1016/j.atmosres.2022.106188.

Pedregosa, F., and Coauthors, 2011: Scikit-learn: Machine learning in Python. *J. Mach. Learn. Res.*, **12**, 2825–2830, https://doi.org/10.48550/arXiv.1201.0490.

Pereira Filho, A. J., F. Vemado, and H. A. Karam, 2019: Evidence of tornadoes and microbursts in São Paulo state, Brazil: A synoptic and mesoscale analysis. *Pure Appl. Geophys.*, **176**, 5079–5106, https://doi.org/10.1007/s00024-019-02276-3.

Piersante, J. O., K. L. Rasmussen, R. S. Schumacher, A. K. Rowe, and L. A. McMurdie, 2021: A synoptic evolution comparison of the smallest and largest MCSs in subtropical South America between spring and summer. *Mon. Wea. Rev.*, **149**, 1943–1966, https://doi.org/10.1175/MWR-D-20-0208.1.

Piscitelli, F. M., J. J. Ruiz, P. Negri, and P. Salio, 2022: A multiyear radar-based climatology of supercell thunderstorms in central-eastern Argentina. *Atmos. Res.*, **277**, 106283, https://doi.org/10.1016/j.atmosres.2022.106283.

Potvin, C. K., K. L. Elmore, and S. J. Weiss, 2010: Assessing the impacts of proximity sounding criteria on the climatology of significant tornado environments. *Wea. Forecasting*, **25**, 921–930, https://doi.org/10.1175/2010WAF2222368.1.

Prein, A. F., and G. J. Holland, 2018: Global estimates of damaging hail hazard. *Wea. Climate Extremes*, **22**, 10–23, https://doi.org/10.1016/j.wace.2018.10.004.

Púčik, T., P. Groenemeijer, D. Rýva, and M. Kolář, 2015: Proximity soundings of severe and nonsevere thunderstorms in central Europe. *Mon. Wea. Rev.*, **143**, 4805–4821, https://doi.org/10.1175/MWR-D-15-0104.1.

——, and Coauthors, 2017: Future changes in European severe convection environments in a regional climate model ensemble. *J. Climate*, **30**, 6771–6794, https://doi.org/10.1175/JCLI-D-16-0777.1.

Rädler, A. T., P. Groenemeijer, E. Faust, and R. Sausen, 2018: Detecting severe weather trends using an additive regressive convective hazard model (AR-CHaMo). *J. Appl. Meteor. Climatol.*, **57**, 569–587, https://doi.org/10.1175/JAMC-D-17-0132.1.

Rasmussen, E. N., and D. O. Blanchard, 1998: A baseline climatology of sounding-derived supercell and tornado forecast parameters. *Wea. Forecasting*, **13**, 1148–1164, https://doi.org/10.1175/1520-0434(1998)013<1148:ABCOSD>2.0.CO;2.

Rasmussen, K. L., and R. A. Houze Jr., 2011: Orogenic convection in subtropical South America as seen by the TRMM satellite. *Mon. Wea. Rev.*, **139**, 2399–2420, https://doi.org/10.1175/MWR-D-10-05006.1.

——, M. D. Zuluaga, and R. A. Houze Jr., 2014: Severe convection and lightning in subtropical South America. *Geophys. Res. Lett.*, **41**, 7359–7366, https://doi.org/10.1002/2014GL061767.

Ribeiro, B. Z., and M. E. Seluchi, 2019: A climatology of quasi-linear convective systems and associated synoptic-scale environments in southern Brazil. *Int. J. Climatol.*, **39**, 857–877, https://doi.org/10.1002/joc.5847.

——, L. A. T. Machado, J. H. Huamán Ch., T. S. Biscaro, E. D. Freitas, K. W. Mozer, and S. J. Goodman, 2019: An evaluation of the *GOES-16* rapid scan for nowcasting in southeastern Brazil: Analysis of a severe hailstorm case. *Wea. Forecasting*, **34**, 1829–1848, https://doi.org/10.1175/WAF-D-19-0070.1.

Romanic, D., M. Taszarek, and H. Brooks, 2022: Convective environments leading to microburst, macroburst and downburst events across the United States. *Wea. Climate Extremes*, **37**, 100474, https://doi.org/10.1016/j.wace.2022.100474.

Romatschke, U., and R. A. Houze Jr., 2010: Extreme summer convection in South America. *J. Climate*, **23**, 3761–3791, https://doi.org/10.1175/2010JCLI3465.1.

Salio, P., M. Nicolini, and E. J. Zipser, 2007: Mesoscale convective systems over southeastern South America and their relationship with the South American low-level jet. *Mon. Wea. Rev.*, **135**, 1290–1309, https://doi.org/10.1175/MWR3305.1.

Schumacher, R. S., and Coauthors, 2021: Convective-storm environments in subtropical South America from high-frequency soundings during RELAMPAGO-CACTI. *Mon. Wea. Rev.*, **149**, 1439–1458, https://doi.org/10.1175/MWR-D-20-0293.1.

Sherburn, K. D., and M. D. Parker, 2014: Climatology and ingredients of significant severe convection in high-shear, low-CAPE environments. *Wea. Forecasting*, **29**, 854–877, https://doi.org/10.1175/WAF-D-13-00041.1.

Silva Dias, M. A. F., 2011: An increase in the number of tornado reports in Brazil. *Wea. Climate Soc.*, **3**, 209–217, https://doi.org/10.1175/2011WCAS1095.1.

Smith, B. T., T. E. Castellanos, A. C. Winters, C. M. Mead, A. R. Dean, and R. L. Thompson, 2013: Measured severe convective wind climatology and associated convective modes of thunderstorms in the contiguous United States, 2003–09. *Wea. Forecasting*, **28**, 229–236, https://doi.org/10.1175/WAF-D-12-00096.1.

Stull, R., 2000: *Meteorology for Scientists and Engineers*. 3rd ed. Brooks/Cole, 502 pp.

Tang, B. H., V. A. Gensini, and C. R. Homeyer, 2019: Trends in United States large hail environments and observations. *npj Climate Atmos. Sci.*, **2**, 45, https://doi.org/10.1038/s41612-019-0103-7.

Taszarek, M., H. E. Brooks, and B. Czernecki, 2017: Sounding-derived parameters associated with convective hazards in Europe. *Mon. Wea. Rev.*, **145**, 1511–1528, https://doi.org/10.1175/MWR-D-16-0384.1.

——, ——, ——, P. Szuster, and K. Fortuniak, 2018: Climatological aspects of convective parameters over Europe: A comparison of ERA-interim and sounding data. *J. Climate*, **31**, 4281–4308, https://doi.org/10.1175/JCLI-D-17-0596.1.

——, and Coauthors, 2019: A climatology of thunderstorms across Europe from a synthesis of multiple data sources. *J. Climate*, **32**, 1813–1837, https://doi.org/10.1175/JCLI-D-18-0372.1.

——, J. T. Allen, T. Púčik, K. A. Hoogewind, and H. E. Brooks, 2020: Severe convective storms across Europe and the United States. Part II: ERA5 environments associated with lightning, large hail, severe wind, and tornadoes. *J. Climate*, **33**, 10 263–10 286, https://doi.org/10.1175/JCLI-D-20-0346.1.

——, N. Pilguj, J. T. Allen, V. Gensini, H. E. Brooks, and P. Szuster, 2021: Comparison of convective parameters derived from ERA5 and MERRA-2 with sounding data over Europe and North America. *J. Climate*, **34**, 3211–3237, https://doi.org/10.1175/JCLI-D-20-0484.1.

Thompson, R. L., B. T. Smith, J. S. Grams, A. R. Dean, and C. Broyles, 2012: Convective modes for significant severe thunderstorms in the contiguous United States. Part II: Supercell and QLCS tornado environments. *Wea. Forecasting*, **27**, 1136–1154, https://doi.org/10.1175/WAF-D-11-00116.1.

Vallis, M. B., A. M. Loredo-Souza, V. Ferreira, and E. L. Nascimento, 2019: Classification and identification of synoptic and non-synoptic extreme wind events from surface observations in South America. *J. Wind Eng. Ind. Aerodyn.*, **193**, 103963, https://doi.org/10.1016/j.jweia.2019.103963.

Varble, A. C., and Coauthors, 2021: Utilizing a storm-generating hotspot to study convective cloud transitions: The CACTI experiment. *Bull. Amer. Meteor. Soc.*, **102**, E1597–E1620, https://doi.org/10.1175/BAMS-D-20-0030.1.

Varga, A. J., and H. Breuer, 2022: Evaluation of convective parameters derived from pressure level and native ERA5 data and different resolution WRF climate simulations over central Europe. *Climate Dyn.*, **58**, 1569–1585, https://doi.org/10.1007/s00382-021-05979-3.

Vera, C., and Coauthors, 2006: The South American Low-Level Jet Experiment. *Bull. Amer. Meteor. Soc.*, **87**, 63–78, https://doi.org/10.1175/BAMS-87-1-63.

Wilks, D. S., 2011: *Statistical Methods in the Atmospheric Sciences*. 3rd ed. International Geophysics Series, Vol. 100, Academic Press, 704 pp.

Zhou, Z., Q. Zhang, J. T. Allen, X. Ni, and C.-P. Ng, 2021: How many types of severe hailstorm environments are there globally? *Geophys. Res. Lett.*, **48**, e2021GL095485, https://doi.org/10.1029/2021GL095485.

Zipser, E. J., D. J. Cecil, C. Liu, S. W. Nesbitt, and D. P. Yorty, 2006: Where are the most intense thunderstorms on Earth? *Bull. Amer. Meteor. Soc.*, **87**, 1057–1072, https://doi.org/10.1175/BAMS-87-8-1057.